

# Research article

## Measurement of atmospheric black carbon in some South Mediterranean cities: Seasonal variations and source apportionment

Hamza Merabet<sup>ID\*1,2</sup>, Rabah Kerbachi<sup>2</sup>, Nikolaos Mihalopoulos<sup>ID 3,4</sup>, Iasonas Stavroulas<sup>4,5</sup>, Maria Kanakidou<sup>ID 4</sup> and Noureddine Yassaa<sup>ID 1,6</sup>

<sup>1</sup>Centre de Développement des Energies Renouvelables, CDER, BP. 62 Route de l'Observatoire Bouzaréah16340 Algiers, Algeria, h.merabet@cder.dz, n.yassaa@cder.dz

<sup>2</sup>Laboratoire des Sciences et Techniques de l'Environnement, Ecole Nationale Polytechnique, 10, Hassan Badi Avenue, El Harrach, Algiers, Algeria, r\_kerbachi@yahoo.fr

<sup>3</sup>Institute of Environmental Research and Sustainable Development (IERSD), National Observatory of Athens (NOA), Athens 152 36, Greece, mihalo@uoc.gr

<sup>4</sup>Environmental Chemistry Processes Laboratory, Department of Chemistry, University of Crete, Heraklion, P.O. Box 2208, 70013, Greece, mariak@uoc.gr

<sup>5</sup>Energy Environment and Water Research Center, The Cyprus Institute, Nicosia 2121, Cyprus, stajas@gmail.com

<sup>6</sup>Laboratoire d'Analyse Organique Fonctionnelle, Faculté de Chimie, Université des Sciences et de la Technologie Houari Boumediene, BP 32, El-Alia, Bab-Ezzouar, 16111 Alger, Algérie.  
Corresponding author, e-mail: h.merabet@cder.dz

Received: 12 April 2019 - Reviewed: 4 June 2019 - Accepted: 10 September 2019

<https://doi.org/10.17159/caj/2019/29/2.7500>

### Abstract

This study aims to investigate, for the first time in Algeria, the atmospheric black carbon (BC) concentrations over one year measured at the Scientific Observatory of Algiers and to compare their concentration levels with other Mediterranean cities (i.e., Athens and Crete). The diurnal cycles as well as seasonal variations of BC concentrations were evaluated and attributed to their emission sources (fossil fuel:  $BC_{ff}$  and wood burning:  $BC_{wb}$ ). The annual mean concentrations of BC,  $BC_{ff}$  and  $BC_{wb}$  were  $1.113 \pm 2.030$ ,  $1.064 \pm 2.002$  and  $0.049 \pm 0.262 \mu\text{g m}^{-3}$ , respectively. The highest seasonal mean concentrations were recorded in summer and autumn with  $1.283 \pm 1.346$  and  $1.209 \pm 1.149 \mu\text{g m}^{-3}$  for BC and  $1.217 \pm 1.431$  and  $1.177 \pm 1.151 \mu\text{g m}^{-3}$  for  $BC_{ff}$ , respectively. However, the lowest mean concentrations were recorded in winter and spring with  $1.023 \pm 1.189$  and  $0.966 \pm 0.964 \mu\text{g m}^{-3}$  for BC and  $0.933 \pm 1.177$  and  $0.956 \pm 0.874 \mu\text{g m}^{-3}$  for  $BC_{ff}$ , respectively. For  $BC_{wb}$ , the highest mean concentrations were reached in winter and summer with  $0.090 \pm 0.055$  and  $0.066 \pm 0.050 \mu\text{g m}^{-3}$ , respectively, very likely due to the forest fires and long-range transport of air pollution from Europe. The lowest mean concentrations of  $BC_{wb}$  were recorded in autumn and spring with  $0.032 \pm 0.033$  and  $0.010 \pm 0.021 \mu\text{g m}^{-3}$ , respectively. Segregating BC levels into eight wind sectors, showed that the prevailing BC pollution with concentrations reaching up to  $5.000 \mu\text{g m}^{-3}$  originated from the North-West wind sector. A source apportionment of BC for the wet and dry period was also performed followed by a back trajectory cluster analysis for long-range transport.

### Keywords

Aerosol, black carbon, atmospheric pollution, source apportionment, seasonal variation, year modulation.

### Introduction

Anthropogenic emissions of aerosols in the atmosphere have increased historically affecting air quality, human health and regional radiative forcing (Seinfeld and Pandis, 2006). Soot or black carbon (BC) is considered a reliable indicator of air pollution at a regional scale (Streets et al., 2001). Because of

its submicron diameter, BC is capable of provoking numerous respiratory diseases and impacting the cardiovascular system, penetrating deep into the lungs and being deposited on the pulmonary alveoli (Cheng et al., 2014). Black carbon plays a great role in the climate system and is responsible for direct and semi-direct effects on regional and global climate (Bond et al.,

2013; Wang et al., 2015) as it absorbs solar radiation and affects the thermal stability of the atmosphere and precipitation (Jose et al., 2016). BC includes elemental carbon (EC, present as graphite), the dominant light absorbing material, that is generally co-emitted and coated by polycyclic aromatic hydrocarbons and humic-like substances or brown carbons (Andreae and Gelencser., 2006).

In addition, once emitted into the atmosphere, BC is subject to atmospheric aging that leads to particles of aged BC that are internally mixed with soluble components such as sulfates or nitrates and also water soluble organics, which increase aerosol solubility (Jennings et al., 1996). Such particles (aged BC) can contribute to the number concentrations of cloud condensation nuclei (CCN) (Bahadur et al., 2012).

Furthermore, during rainfall the fresh BC, which is not hygroscopic, can be removed from the atmosphere by wet scavenging (below-cloud scavenging), while aged hygroscopic BC particles can be removed both by in-cloud and below-cloud scavenging due to condensation of secondary inorganic aerosols on BC (Gadhavi and Jayaraman, 2010).

The physical and chemical properties of aerosols change significantly when BC is mixed with dust aerosols during dust events (Pu et al., 2015). The binding of organic pollutant particles with BC influences their transport and limits their bioavailability (Ali et al., 2014). It was proved that BC adsorbs strongly to pesticides, polycyclic aromatic hydrocarbons (PAHs), biphenyls (PCBs) and polychlorinated dibenz-p-dioxins (PCDDs), which can exacerbate water and soil pollution and human disease (Lohmann et al., 2005). BC can travel hundreds to thousands of kilometers in the atmosphere, but in sediments, it can live up to several millions of years (Masiello and Druffel, 1998). During monsoon season, low BC concentrations are associated with higher wind speeds and rainfall (Begam et al., 2016). The diurnal evolution of the atmospheric boundary layer (ABL) is a determinant factor for the variation of BC concentrations during the nighttime (Nair et al., 2007). The surface heating during the daytime increases the ABL height and results in a dilution of atmospheric aerosols in the ABL, thus decreasing BC concentration (Jose et al., 2016). In Algeria, similarly to other southern Mediterranean countries, no detailed studies of BC levels have been reported to date, to the best of our knowledge. The present study aims to document, for the first time, BC air pollution in Algiers through a full year of BC measurement performed at the observatory of Algiers from 1 June 2014 to 31 May 2015.

## Experimental

### Description of the measurement site

The sampling station is located at the Scientific Observatory of Bouzaréah, Algiers at the Centre de Développement des Energies Renouvelables (CDER). The site is situated at 36.8°N, 3.0°E, at 345m above the sea level in the highest Algiers plateau

and at about 1 km from the Mediterranean Sea coast. It is also located about 6 km to the north-west of the Algiers downtown and has no significant industrial and agricultural combustion activities surrounding the sampling site at a distance of several kilometers; however, there is a forest about 3 km to the west (see Figure 1).

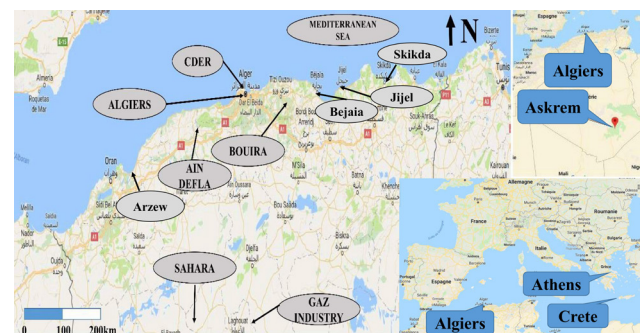


**Figure 1:** Location of investigated sampling site.

## Instruments

### Aethalometer

From 1 June 2014 to 31 May 2015, continuous BC observations have been performed at a height of 3m above ground level using an aethalometer (model AE-33 of Magee Scientific, USA).

The aethalometer AE33 instrument measures the light beam attenuation in seven wavelengths (370, 470, 520, 590, 660, 880 and 950 nm), operating with a flow rate of 5 L/min, a 1-minute measurement interval and an automatic zero calibration with an accuracy of 0.001  $\mu\text{g m}^{-3}$ . According to the manufacturer, the instrument sensitivity is 0.03  $\mu\text{g m}^{-3}$  at 1 minute and its detection limit is 0.005  $\mu\text{g m}^{-3}$  for a 1-hour mean. The aethalometer uses the patented Dual Spot method to compensate for the 'spot loading effect' and provides a real-time output of the 'loading compensation' parameter, which may provide additional information about the physical and chemical properties of the aerosol (aethalometer Model AE33, user manual). The aethalometer AE33 used in the present study is equipped with a sampling head, which has an inlet with a diameter allowing the entry of  $\text{PM}_{2.5}$ . The BC measured in the present study was obtained by the following equation.

$$\text{BC}_{\text{reported}} = \text{BC}_{\text{zeroloading}} * (1 - k * \text{ATN}) \quad (1)$$

where  $\text{BC}_{\text{reported}}$  is the BC measured by the aethalometer,  $\text{BC}_{\text{zeroloading}}$  is the BC measured by the instrument without loading effect,  $k$  is the loading compensation parameter, and ATN is the attenuation of light beam in the wavelength of measurement. The equations below are taken from the aethalometer model developed by Scire et al., (2011). Aerosol absorption coefficients ( $b_{\text{abs}}$ ) were obtained by equations 2 and 3.

$$b_{\text{abs}, 470\text{nm}} = \text{BC}_{470\text{nm}} * 14.54 / 1000 \quad (2)$$

$$b_{abs,950nm} = BC_{950nm} * 7.19 / 1000 \quad (3)$$

where 14.54 and 7.19 are the Mass Absorption Efficiency (MAE) in the two wavelengths, 470nm and 950nm, respectively, and are provided by the manufacturer. We used the measurements at 470nm in order to avoid the absorption by the dust at 370nm. The equations 4 to 7 enabled the calculation of the  $BC_{ff}$  (fossil fuel) and  $BC_{wb}$  (wood burning).

$$b_{abs,\lambda} = b_{abs,ff,\lambda} + b_{abs,wb,\lambda} \quad (4)$$

$$b_{abs,ff,470nm} / b_{abs,ff,950nm} = (470 / 950)^{-\alpha_{ff}} \quad (5)$$

$$b_{abs,wb,470nm} / b_{abs,wb,950nm} = (470 / 950)^{-\alpha_{wb}} \quad (6)$$

$$BC_{ff} = BC * b_{abs,ff,950nm} / b_{abs,950nm} \quad (7)$$

where  $b_{abs,\lambda}$  is the light absorption coefficient at the wavelength  $\lambda$  (we used 950nm wavelength),  $b_{abs,ff,\lambda}$  is the light absorption coefficient for the  $BC_{ff}$  and  $b_{abs,wb,\lambda}$  is the light absorption coefficient of  $BC_{wb}$ ,  $\alpha_{ff}$  and  $\alpha_{wb}$  are the Angstrom exponents for fossil fuel and wood burning in Algiers, respectively. The  $\alpha_{ff}$  and  $\alpha_{wb}$  calculated by Sciare et al. (2011) were equal to 1 and 2 respectively. The combination of these equations using dedicated software developed by Sciare et al. (2011) was applied for the calculation of  $BC_{ff}$  and  $BC_{wb}$ . In addition to BC, biomass-burning aerosols contain a substantial fraction of organic substances, which absorb in the N-UV and blue part of the spectrum in contrast to the N-IR wavelength range, resulting in  $\alpha_{wb}$  larger than  $\alpha_{ff}$  (Zotter et al., 2017). It is also important to mention that BC exists in mixed nature (from fossil fuel and wood burning at the same time).

A calculation of the mass absorption cross-section (MAC) has been performed in this study by using the following equation:

$$\sigma_{air} = \frac{S * (\Delta ATN / 100)}{BC * Fin \Delta t * C} \quad (8)$$

where, S=spot size; t=time, C=multiple scattering parameter (Weingartner et al., 2003),  $\sigma_{air}$ =mass absorption crossection.

$$Fin = Fout * (1 - \zeta) \quad (9)$$

where,  $Fout$ =measured flow,  $\zeta$ =leakage factor.

$$ATN = -100 * \ln\left(\frac{I}{I_0}\right) \quad (10)$$

Where,  $I_0$ =reference signal and  $I$ =spot signal.

### Meteorological data

Local meteorological parameters such as air temperature, relative humidity, wind speed and direction, atmospheric pressure and rain intensity were monitored by the CHEMS network of the CDER (composed of a weather and radiometric station) at 5-minute intervals using instruments situated near the aethalometer.

### Traffic informations

Two national roads exist near the site about 1 km to the north and about 2km to the east, and roads with light traffic are about 200m to the south-east and 1.5 km to the west of the monitoring site. These roads can be sources of BC emissions. Algiers's car fleet includes more than 1,400,000 vehicles of all categories, with 31.32% using diesel and 68.68% using petrol as of the end of 2014, and about 1 million cars coming daily from the other regions. The car fleet in Algeria is old (51.11% of vehicles' age is greater than 20 years) (<http://www.ons.dz/Au-31-12-2014-.html>) and has more than 5,000,000 cars of all categories, with 34.29% powered by diesel versus 65.71% by petrol. Almost all goods are transported by road. Algiers has also a train station, a harbor, an airport, and an industrial area situated at about 4, 5, 25 and 20 km from the measurement site, respectively.

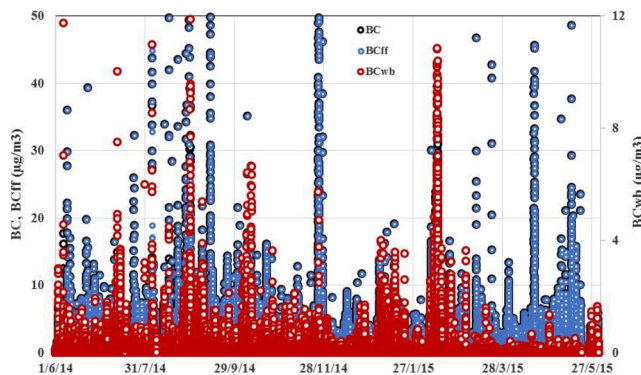
## Results and discussion

### Monitoring of black carbon

One-year observations of BC,  $BC_{ff}$  and  $BC_{wb}$  with hourly, diurnal, and seasonal evolutions allow better understanding of high pollution events due to the rush hour traffic emissions, wild fires, oil industry to the south, celebration events (coinciding with high BC emissions due to abusive use of pyrotechnic products) and long-range air pollution transport from Europe or neighboring countries.

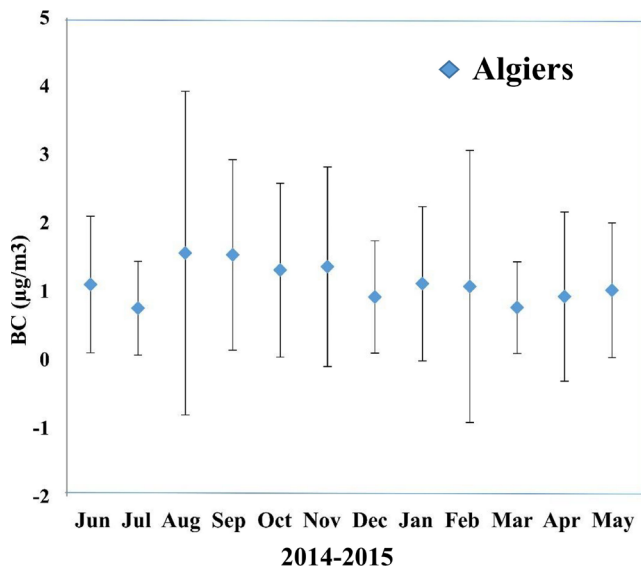
### Black carbon variability

Figure 2 presents BC concentrations recorded at the scientific observatory of Bouzaréah (from 1 June 2014 to 31 May 2015), along with  $BC_{ff}$  and  $BC_{wb}$  calculated for the site. The BC concentrations were recorded at 950 nm wavelength, and the missing data are indicated with blanks. The equal distance between the high peaks is explained by the moving of the tape roll when the attenuation (ATN) at 370 nm reaches 100 (Sciare et al., 2011), which leaves gaps of two to three minutes. BC and  $BC_{ff}$  concentration levels were high with several peaks reaching 50.000  $\mu\text{gm}^{-3}$ , however,  $BC_{wb}$  values were low and usually close to 0  $\mu\text{gm}^{-3}$ . The BC,  $BC_{ff}$  and  $BC_{wb}$  mean concentrations were  $1.113 \pm 2.030$ ,  $1.064 \pm 2.002$  and  $0.049 \pm 0.262 \mu\text{gm}^{-3}$ , respectively. It is worth noting that the  $BC_{ff}$  represents 95.60% of BC total concentration mass, suggesting that the main BC pollution originated from fossil fuel (traffic and oil industry). It is important to mention that the main source of heating in Algiers and in Algeria in general is natural gas, which is also the principal source of electricity production (96%). Therefore, the predominant  $BC_{ff}$  emissions are diesel, gasoline and kerosene used in the transport sector.



**Figure 2:** One-year of BC, BC<sub>ff</sub> and BC<sub>wb</sub> measurements.

The monthly averages of BC varied between  $0.759 \pm 0.669$  and  $1.556 \pm 2.366 \mu\text{gm}^{-3}$  as presented in the Figure 3. The results are close to the previous ones presented in the Figure 2 with large standard deviation values due to the huge quantity of results treated in the present study.



**Figure 3:** Variation of monthly BC averages and standard deviations during the year of measurement.

The daily peaks of BC exceeding  $5.000 \mu\text{gm}^{-3}$  could be related to forest fires or a regional source (heating) which can be confirmed by the BC<sub>wb</sub> concentrations, e.g., on 29 August 2014, the mean concentration of BC<sub>wb</sub> from 02:00 to 09:00 was  $0.450 \mu\text{gm}^{-3}$ . On 4 August 2014, BC<sub>wb</sub> mean concentration from 04:00 to midnight (00:00) was  $0.180 \mu\text{gm}^{-3}$  and on 7 September 2014, BC<sub>wb</sub> mean concentration from midnight (00:00) to 15:00 was  $0.055 \mu\text{gm}^{-3}$ . The yearly percentage of BC<sub>ff</sub> was very high (95.60%), compared to BC<sub>wb</sub> (4.40%). This result revealed that the main sources of BC in Algeria are local activities and road traffic rather than forest fires and cooking.

These results could be of great importance for air quality management policy. The measured BC concentrations can be compared with literature data from other locations as presented in Table 1. The annual average of BC recorded at

the Algiers Observatory was much lower than that recorded in Anantapur (India), Prague (Czech), Athens (Greece) and Rome (Italy). In contrast, it was higher than measured values in Santa Cruz de Tenerife (Spain), Crete (Greece) and Finland. Chiloane et al., (2017) recorded BC mean concentrations ranging between  $0.7$  and  $1.4 \mu\text{gm}^{-3}$  in background sites and sites influenced by industrial activities and/or nearby settlements in South Africa.

A thorough investigation of BC variation in the present study is needed for a comparison and characterization in order to explain these findings.

The highest seasonal mean concentrations of BC, BC<sub>ff</sub> and BC<sub>wb</sub> were recorded in summer with  $1.283 \pm 1.346$ ,  $1.217 \pm 1.431$  and  $0.066 \pm 0.050 \mu\text{gm}^{-3}$ , respectively, which could be explained by the scarcity of rains and winds on the one hand and the increase of visitors to the north of Algeria during summer holidays on the other hand. The high BC<sub>wb</sub> levels in summer are attributed to the forest fires recorded during that season.

The second most polluted season was the autumn, where mean concentrations reaching  $1.209 \pm 1.149 \mu\text{gm}^{-3}$  for BC and  $1.177 \pm 1.151 \mu\text{gm}^{-3}$  for BC<sub>ff</sub> were recorded, explained by the intensive socioeconomic activity started after the summer holidays which is reflected by the traffic road increase, however, the BC<sub>wb</sub> mean concentration was lower at  $0.032 \pm 0.033 \mu\text{gm}^{-3}$  due to the decrease of the magnitude of forest fires during this season, and the low use of wood burning in Europe. During winter, the mean concentrations of BC and BC<sub>ff</sub> were lower than in autumn ( $1.023 \pm 1.189$  and  $0.933 \pm 1.177 \mu\text{gm}^{-3}$ , respectively); however, the BC<sub>wb</sub> mean concentration was the highest at  $0.090 \pm 0.055 \mu\text{gm}^{-3}$ , which can be related to air masses originating from Europe and having a high BC<sub>wb</sub> load (due to domestic heating emissions).

During spring, the mean BC, BC<sub>ff</sub> and BC<sub>wb</sub> concentrations were the lowest with  $0.966 \pm 0.964$ ,  $0.956 \pm 0.874$  and  $0.010 \pm 0.021 \mu\text{gm}^{-3}$ , respectively, attributed to air masses coming mostly from the north-west, with low BC<sub>wb</sub> from Europe (low use of wood and coal for heating in spring), south, and local sources with a very high rate of BC<sub>ff</sub> (98.96%) due to petroleum industry and traffic.

For the sake of comparison, Table 2 reports the seasonal variations of BC measured in this study and those reported in the literature.

The mean concentrations of BC recorded in the present study during summer was higher than those measured in Prague (Czech) and Mahabaleshwar (India). In contrast, the BC concentrations measured in this study were lower than mean concentrations documented for six large Brazilian cities. The results recorded in winter are higher than those measured in Paris and Toulouse, but lower than the mean concentrations obtained in Cairo (Egypt), Prague (Czech Republic) and six large Brazilian cities. For the spring season, the concentration levels were higher than those reported in Stockholm (Sweden), but, lower than the mean concentrations recorded in Prague and

**Table 1:** Comparison of [BC] (in  $\mu\text{g m}^{-3}$ ) measured in the present study and other concentrations reported in the literature.

Station	Type of site	BC Concentration	Period	Reference
Algiers (Algeria)	Suburban	1.113±2.030	June 2014–May 2015	Present study
Hyderabad (India)	Urban	15.91	March (2010–2012)	(Jose et al. 2016)
Hyderabad (India)	Urban	9.84	June (2010–2012)	(Jose et al. 2016)
Anantapur (India)	Semi-arid, Suburban	3.03		(Reddy et al., 2012)
Indian Himalayas	Background	0.90±0.60	2005–2014	(Hooda et al., 2018)
Prague (Czech)	Suburban	1.71	Sep 2009–Aug 2010	(Vodička et al. 2013)
Barcelona (Spain), Lugano (Switzerland), London, and North Kensington (England)	Urban background	1.7–1.9	2009	(Reche et al. 2011)
London, Marylebone (England)	Urban traffic	7.8	2009	(Reche et al., 2011)
Bern (Switzerland)	Urban traffic	3.5	2009	(Reche et al., 2011)
New York(USA)	Urban	1.38	Jan–Feb 2004	(Venkatachari et al., 2006)
Mexico City(Mexico)	Urban	3.4	Apr 2003	(Salcedo et al., 2006)
Hong Kong (China)	Coastal rural	2.4	Jun 2004–May 2005	(Cheng et al., 2006)
Huelva (Spain)	Urban background	0.7	2009	(Reche et al., 2011)
Santa Cruz de Tenerife (Spain)	Urban background	0.8	2009	(Reche et al., 2011)
Finland	Urban	1.71	Sep 2009–Aug 2010	(Saarikoski et al., 2008)
Baltic Sea	Coastal rural	0.6	2008–2009	(Byčenkienė et al., 2011)
South of China	Oceanic site	0.28–2.14	Daily BC averages	(Wu et al., 2013)

**Table 2:** Comparison of seasonal [BC] (in  $\mu\text{g m}^{-3}$ ) measured in the present study and other values reported in the literature.

Station	Type of site	BC Concentration	Season	Reference
Algiers (Algeria)	Suburban	1,283±1.346	Summer	Present study
		1,209±1.149	Autumn	
		1,023±1.181	Winter	
		0,966±0.964	Spring	
Prague (Czech)	Suburban	1.26	Spring	(Vodička et al. 2013)
Prague (Czech)	Suburban	0.87	Summer	(Vodička et al. 2013)
Prague (Czech)	Suburban	2.06	Autumn	(Vodička et al. 2013)
Prague (Czech)	Suburban	2.66	Winter	(Vodička et al. 2013)
Six large Brazilian cities		2.30–7.10	Summer	(De Miranda et al. 2012)
Six large Brazilian cities		4.0–13.1	Winter	(De Miranda et al. 2012)
Stockholm (Sweden)	Rural	0.36	Spring	(Krecl et al. 2011)
Stockholm (Sweden)	Street canyon site	5.39	Spring	(Krecl et al. 2011)
Cairo (Egypt)		9.9	2004 Autumn	(Mahmoud et al. 2008)
Cairo (Egypt)		6.9	2005 Spring	(Mahmoud et al. 2008)
Paris (France)	Suburban site	0.9	Winter	(Laborde et al. 2013)
Toulouse, France	Coastal urban	0.95	2005 Winter	(Saha and Despiau. 2009)
Mahabaleshwar (India)	Rural	0.303	Summer	(Singla et al. 2019)

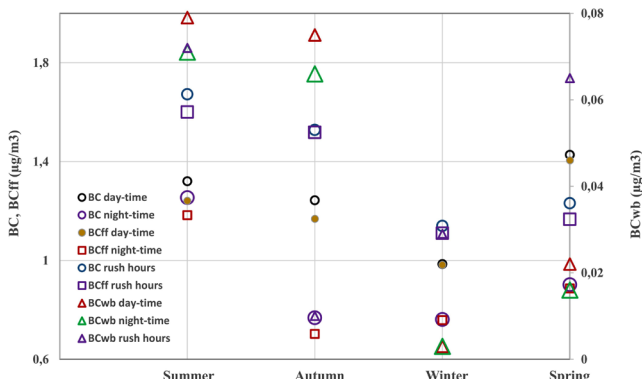


**Figure 4:** Daytimes, nighttimes and rush hours mean concentrations of BC, BC<sub>ff</sub> and BC<sub>wb</sub> quarterly averages.

Cairo. Finally, during autumn, the mean concentrations recorded in Algiers were lower than those measured in Prague (Czech). The difference between the seasonal mean concentrations of BC recorded in Algiers and other cities could depend not only on the national emissions related to wild fires, industry, and transport, but also on the long-range transport pathways which will be studied in the rest of the study.

Figure 4 displays the seasonal variation of the daytime, nighttime and rush hour mean concentrations of BC, BC<sub>ff</sub> and BC<sub>wb</sub>, during the studied one-year period.

It shows that during the daytime, spring was the most polluted season with BC and BC<sub>ff</sub> mean concentrations reaching up to  $1.427 \pm 1.045$  and  $1.405 \pm 1.043 \text{ } \mu\text{gm}^{-3}$ , respectively, followed by the summer season when concentrations of  $1.320 \pm 0.958 \text{ } \mu\text{gm}^{-3}$  for BC and  $1.241 \pm 1.504 \text{ } \mu\text{gm}^{-3}$  for BC<sub>ff</sub> were recorded.

These high mean concentrations of BC with high rates of BC<sub>ff</sub> reaching 98.46% in spring season can be explained by the decrease of rains, the increase of airflow from the south charged with BC<sub>ff</sub> emitted by oil industry and the air masses coming from Europe.

In summer, the rate of BC<sub>ff</sub> concentration was less at 94.00% due to the wild fires emitting BC<sub>wb</sub>. The lowest mean BC and BC<sub>ff</sub> concentrations were recorded in the winter season at  $0.985 \pm 1.409$  and  $0.982 \pm 1.401 \text{ } \mu\text{gm}^{-3}$ , respectively, which can be explained by the wet scavenging by the rain and the dispersion by winds.

During nighttime, summer is the most polluted season by BC and BC<sub>ff</sub> with concentrations of  $1.254 \pm 1.306$  and  $1.183 \pm 1.306 \text{ } \mu\text{gm}^{-3}$ , respectively, followed by the autumn season with  $0.902 \pm 0.779$  and  $0.886 \pm 0.781 \text{ } \mu\text{gm}^{-3}$ , because of the increased use of cars during the night contrary to autumn and winter seasons. It is worth noting that the majority of the industries in Algeria work 24 hours a day, leading to increased emissions of BC<sub>ff</sub> by cars and machines during the night.

As to BC<sub>wb</sub>, the highest mean concentrations were recorded during the summer followed by the autumn with  $0.071 \pm 0.571$

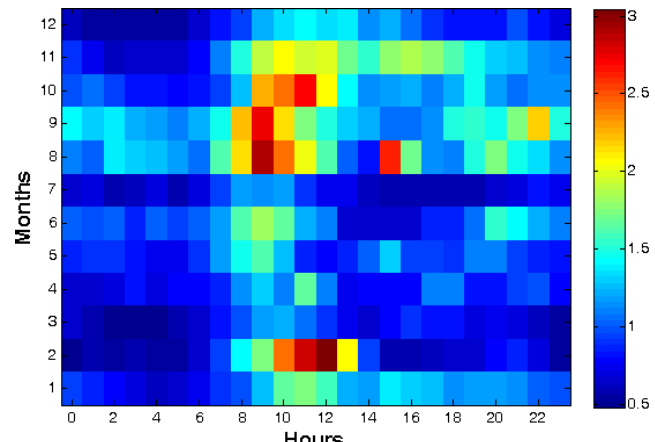


**Figure 5:** Month-hour plot of BC ( $\mu\text{gm}^{-3}$ ) during the year of measurement.

and  $0.066 \pm 0.028 \text{ } \mu\text{gm}^{-3}$  respectively, which is due to the forest fires in summer and wood burning coming from Europe in autumn with a scarcity of rains in Algeria. The lowest BC<sub>wb</sub> was observed in the spring with  $0.003 \pm 0.194 \text{ } \mu\text{gm}^{-3}$ , which can be explained by the wet scavenging by rains and the dispersion by winds.

As the cooking and heating in Algeria is from natural gas, the BC<sub>wb</sub> measured in our study could be due to cooking and heating from Europe and from wild fires during the summer (both in Europe and in Algeria). The BC<sub>wb</sub> in the daytime was higher than BC<sub>wb</sub> at night during summer, autumn and spring, which is due to the fires recorded in Algeria in summer with a higher frequency and magnitude of spread during the day than at night and the low use of heating in Europe during spring and autumn. However, in winter, we recorded in Algiers a similar average of BC<sub>wb</sub> concentration in the daytime and in the nighttime, which could be explained by the long-range transport from Europe with a high use of wood and coal for heating and cooking during the day and the night.

For the BC and BC<sub>ff</sub> average concentrations in rush hours (07:00 and 10:00), summer and autumn were the most polluted with  $1.672 \pm 1.297$  and  $1.528 \pm 1.167 \text{ } \mu\text{gm}^{-3}$  for BC and  $1.600 \pm 1.327$  and  $1.518 \pm 1.171 \text{ } \mu\text{gm}^{-3}$  for BC<sub>ff</sub>, respectively. These concentrations, which were higher than the yearly average, can be explained by the citizens' behavior during peak hours in Algeria: leaving work and school at the same time, and lunch between midday and 13:00 for most citizens. The seasonal maximum levels of BC<sub>wb</sub> during rush hours (between 11:00 and 14:00) were recorded in summer and spring with  $0.381 \pm 0.232$  and  $0.183 \pm 0.151 \text{ } \mu\text{gm}^{-3}$ , respectively, most likely associated with cooking activities in restaurants and wild fires.

In Figure 5, we present the month-hour variation plot of BC during the period of measurement in Algiers as plotted by Hooda et al. (2018). The figure presents better the variation of BC depending on hours and months and completes the previous interpretations. It is clear that the BC peaks were observed in the summer during the rush hours. The BC concentrations during daytimes were very high during spring months, which is

in line with the previous interpretations. The figure summarizes what was presented previously and gives a more precise view of the hourly averages during the months studied.

Figure 6 shows the mean diurnal cycle of BC,  $BC_{ff}$  and  $BC_{wb}$  concentrations during the studied period of one year. The diurnal cycle reflects the combined effect of variations in anthropogenic emissions, surface meteorology and ABL dynamics (Ramachandran and Rajesh, 2007). Targino and Krecl, (2017) reported that local traffic was by far the most important source of BC in street canyon in a mid-sized city in southern Brazil, with hourly mean concentration peaking during the rush hours at  $5.840 \mu\text{g m}^{-3}$  in the morning at 06:00 and at  $4.550 \mu\text{g m}^{-3}$  in the afternoon at 18:00.

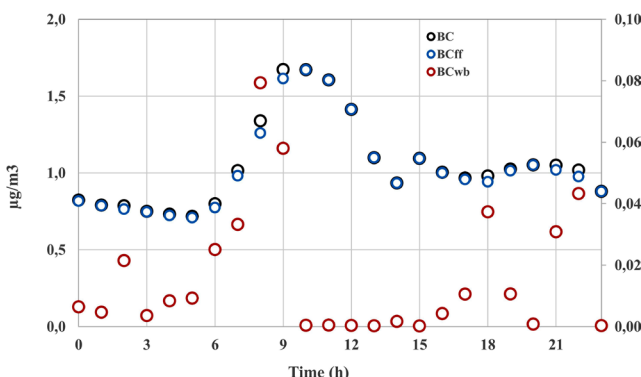


**Figure 6:** Mean diurnal cycle of mean BC,  $BC_{ff}$  and  $BC_{wb}$  concentrations during the year of measurement.

In the present study, the hourly mean concentrations of BC and  $BC_{ff}$  were higher than  $1.300 \mu\text{g m}^{-3}$  between 08:00 and midday (12:00) with maximum concentration of  $1.673 \mu\text{g m}^{-3}$  at 09:00, due to the high traffic. In contrast, the concentrations were as low as  $0.718 \mu\text{g m}^{-3}$  for BC and  $0.709 \mu\text{g m}^{-3}$  for  $BC_{ff}$  at 05:00. For  $BC_{wb}$ , low hourly mean concentrations were recorded with two peaks at 08:00 and 09:00 reaching  $0.079$  and  $0.058 \mu\text{g m}^{-3}$ , respectively, most likely related to the indoor and outdoor cooking and heating.

In Figure 7, a comparison of BC daily variability with the means of wind speed (ws) and recorded rainfall has been presented. An inversely proportional relationship between the wind speed and rainfall on the one hand and BC concentrations on the other hand was observed. A statistical study of daily data revealed a correlation between ws and rainfall increase and BC decrease, which is very clear in Figure 7. When ws was less than  $5 \text{ m s}^{-1}$ , the BC decreased with a good correlation (correlation coefficient  $K=0.16$ ); however, BC concentrations increased with the ws higher than  $5 \text{ m s}^{-1}$ . This result could be explained by the dispersion of BC pollution when winds are moderate. In contrast, the increase of BC when ws is higher than  $5 \text{ m s}^{-1}$  could be due to the atmosphere disruption. Nevertheless, a relationship between rainfall and BC decrease was recorded, with a better correlation when rainfall is less than  $3 \text{ mm}$ . BC dispersion by winds and the wet scavenging by rains can explain the decrease of BC. High wind speed may increase the vertical mixing thereby diluting particles among them black carbon in

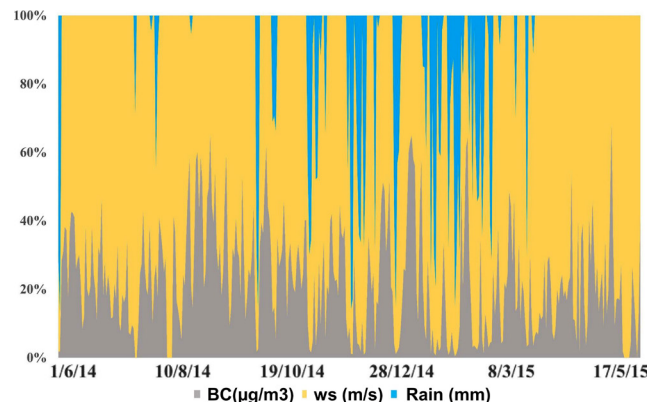


**Figure 7:** BC daily variability with the wind speed (ws) and rainfall during the year of measurement.

addition to the dispersion of BC by winds, which decreases the BC concentrations. Low atmospheric boundary layer height and low wind speeds during winter can be also attributed to high accumulation of BC aerosols (Begam et al., 2016).

To study the relationship between the atmospheric boundary layer (ABL) and BC concentrations, Table 3 presents the averages of BC vs ABL height. Cheng et al. (2014) revealed that the BC mass concentrations decreased during the afternoon hours, due to the boundary layer dynamics and a lower car fleet volume. Begam et al., 2016, confirmed the inverse proportional relationship between the ABL level and BC concentrations. In the present study, it was observed that BC levels were high when the boundary layer was lower than 1000m, and decreases with the ABL height, which is explained by the pressure applied by the ABL on the air pollutants, decreasing the volume and increasing the concentrations.

**Table 3:** Variation of BC averages and Atmospheric Boundary Layer heights.

ABL (m)	BC average ( $\mu\text{g m}^{-3}$ )
1000	1.16
2000	1.10
3000	1.06
4000	1.05
5000	1.05

#### Sources of black carbon

Figures 8a,b,c,d show some pollution events (pollution from the Sahara, sport and religious celebrations, forest fires, long-range transport from Europe as well as a day without cars). The hourly averages of BC,  $BC_{ff}$  and  $BC_{wb}$  concentrations during 7 September 2014 are displayed in Figure 8a. High levels of BC and  $BC_{ff}$  reach  $9.043$  and  $8.996 \mu\text{g m}^{-3}$ , respectively, between 09:00 and 10:00. A high peak of  $BC_{wb}$  reaching  $0.133 \mu\text{g m}^{-3}$  between 10:00 and 11:00 was also measured. These high levels of  $BC_{wb}$  were attributed to the forest fires in Ain Defla in the south-west

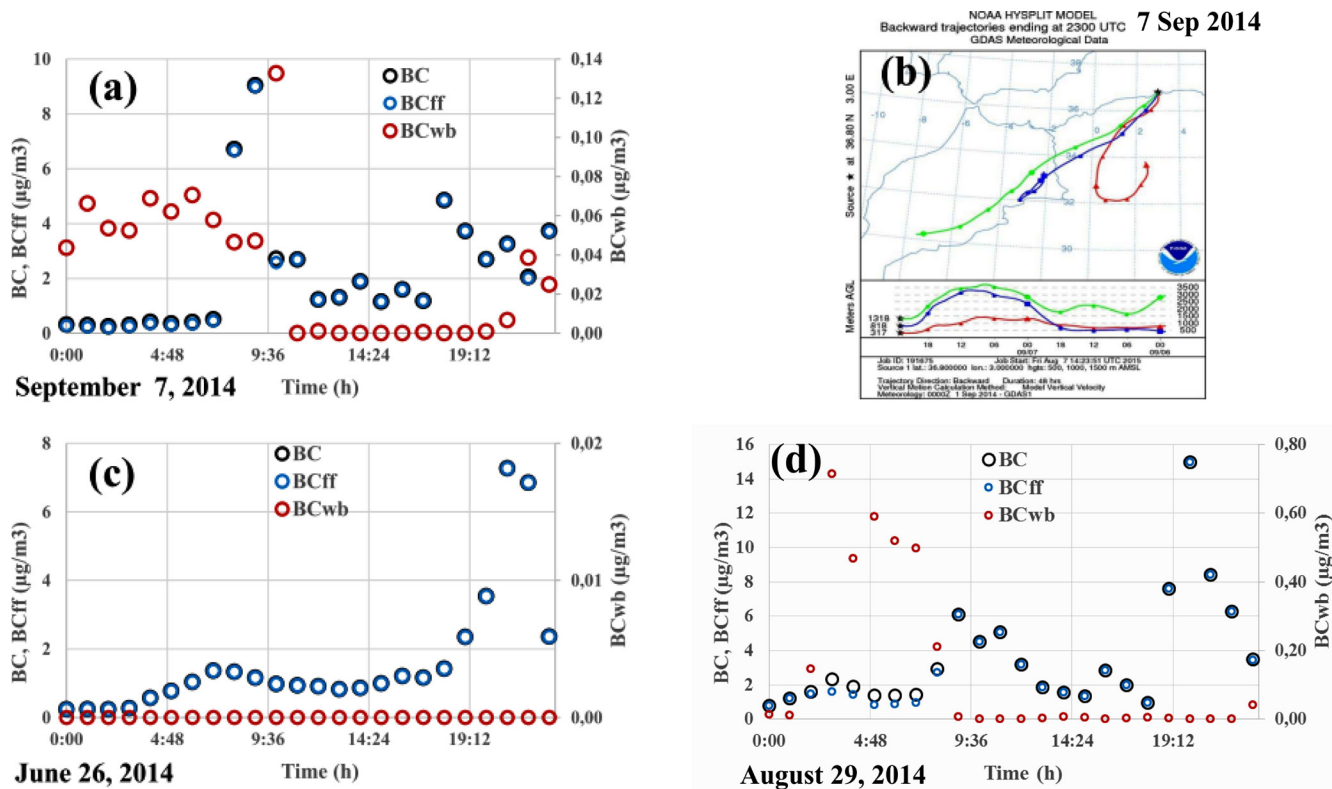


**Figure 8:** Variation of BC, BC<sub>ff</sub> and BC<sub>wb</sub> concentrations on polluted days (7 September, 26 June and 29 August 2014).

of Algiers that occurred during the same period, as cited by the Algerian Directorate General of Forestry, and affecting the region as confirmed by the air mass trajectories shown in Figure 8b. The high levels of BC and BC<sub>ff</sub> can be associated with other air masses coming from the petroleum industry in the Sahara (Figure 8b).

Figure 8c displays the hourly averages of BC, BC<sub>ff</sub> and BC<sub>wb</sub> on 26 June 2014, when the national soccer team of Algeria came for the first time to the second round of the 2014 World Cup. High levels of BC and BC<sub>ff</sub> were recorded during the night of 26 June exceeding 7.000  $\mu\text{g m}^{-3}$  between 21:00 and 23:00 with 98.88% of the BC being BC<sub>ff</sub>. This pollution has been produced by traffic emissions and excessive use of pyrotechnic products exacerbated during this particular celebration event. The hourly averages of BC, BC<sub>ff</sub> and BC<sub>wb</sub> on 29 August 2014 are shown in Figure 8d. High peaks of BC and BC<sub>ff</sub> reached up to 14.000  $\mu\text{g m}^{-3}$  between 20:00 and 21:00 and high levels of BC<sub>wb</sub> reached 0.715  $\mu\text{g m}^{-3}$  between 03:00 and 04:00 and 0.589  $\mu\text{g m}^{-3}$  between 05:00 and 06:00 with a daily mean concentration of 0.199  $\mu\text{g m}^{-3}$ .

The Hysplit back trajectories (Figure 9a) corroborated the occurrence of huge forest fires in the east of Algiers (300 km away) in Bejaia and Jijel, as announced by the Director General of Forestry. The fires started on 27 August 2014 and the plume arrived at Algiers on 29 August 2014. The mean concentrations of BC and BC<sub>ff</sub> between 20:00 and 21:00 were similar and very high (i.e., 14.953  $\mu\text{g m}^{-3}$ ), suggesting the dominance of fossil fuel sources of BC after the extinction of the forest fires. Interestingly, Figure 9b compares the variation of BC in two successive

celebrations years of the Birthday of Muslim Prophet (Mawlid Enabawi) coincided with the nights of 2 January 2015 and 23 December 2015. High levels of BC concentrations were recorded with peaks exceeding 9.000  $\mu\text{g m}^{-3}$  on 23 December and 5.000  $\mu\text{g m}^{-3}$  on 2 January, and daily mean concentrations of 3.477  $\mu\text{g m}^{-3}$  on 23 December, and 0.559  $\mu\text{g m}^{-3}$  on 2 January, occurring during tremendous use of pyrotechnic products. Seidel and Birnbaum (2015) reported an increase of the US-average mean hourly PM<sub>2.5</sub> values reaching 21.000  $\mu\text{g m}^{-3}$  21:00 to 22:00 during the celebration of the national independence day in the US (4 July 1999-2013) and a decrease to zero by noon the day after (5 July 1999-2013). The authorities implemented a day without traffic road in the center of Algiers. This special case helps to assess to what extent the impact of traffic on BC emissions is important for BC levels in the Algiers city. Figure 9c presents a comparison of BC variations between an ordinary day (7 August 2015) and a day without cars in Algiers (31 July 2015).

A substantial drop in BC concentrations of between 47.3% and 92.4% was observed during the day without cars relative to the days with cars, considering that the air mass sources are local during the ordinary (day with cars) day and from the south-west from the region having no oil industry, for the day without cars as shown in Figure 10. The BC average concentrations during the day and the night of this day without cars were 0.564 and 0.543  $\mu\text{g m}^{-3}$ , respectively, representing 50% on the annual average, which demonstrates the role of car fleet in BC levels in Algiers.

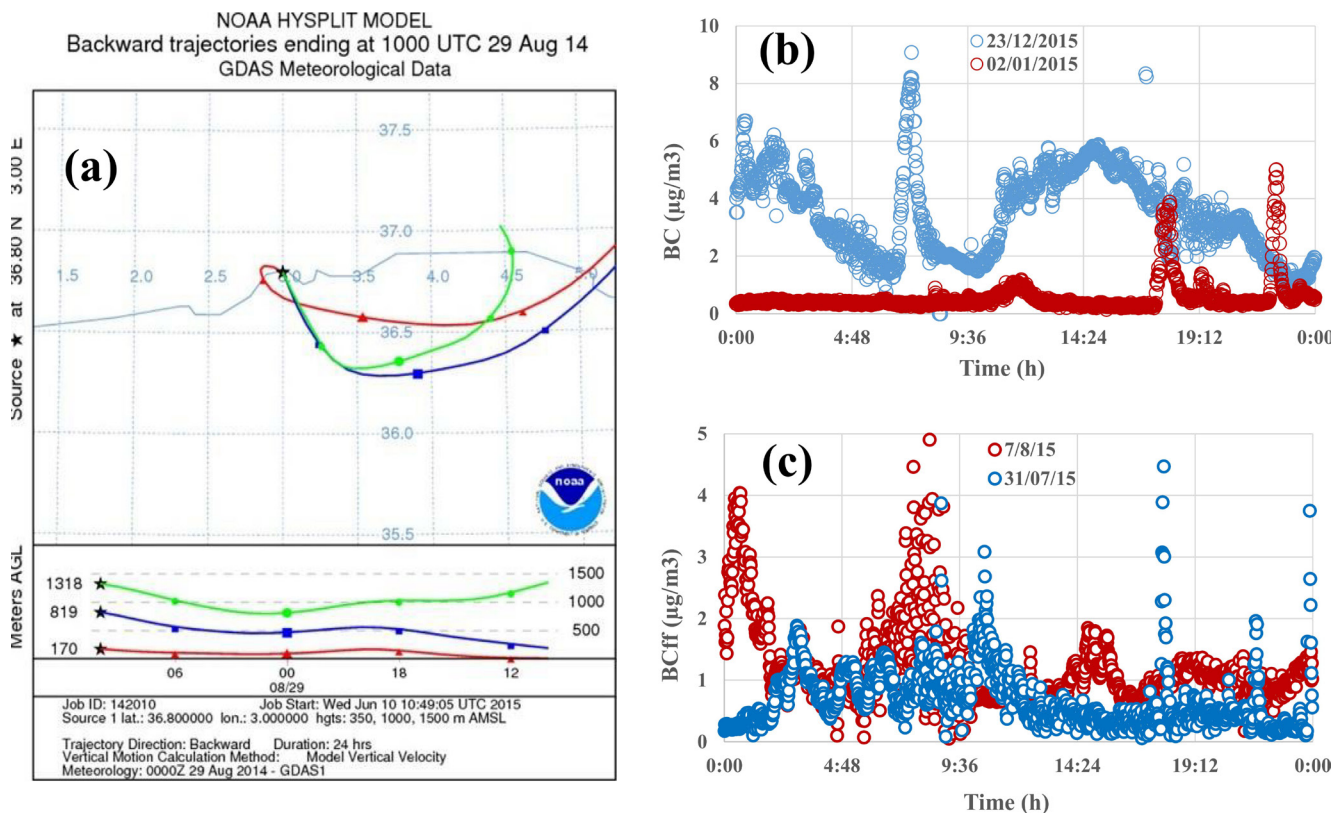


Figure 9: Variation of BC during pollution events (29 August 2014, 2 January, 23 December, 31 July and 7 August 2015).

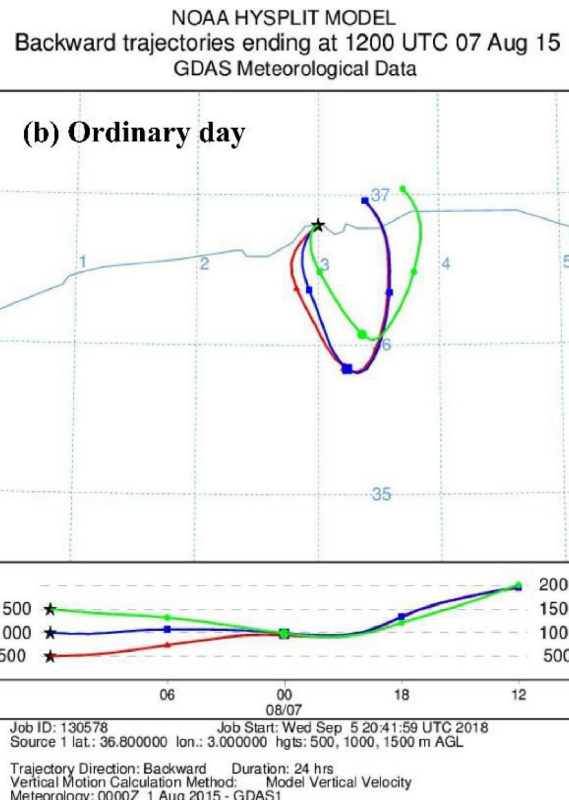
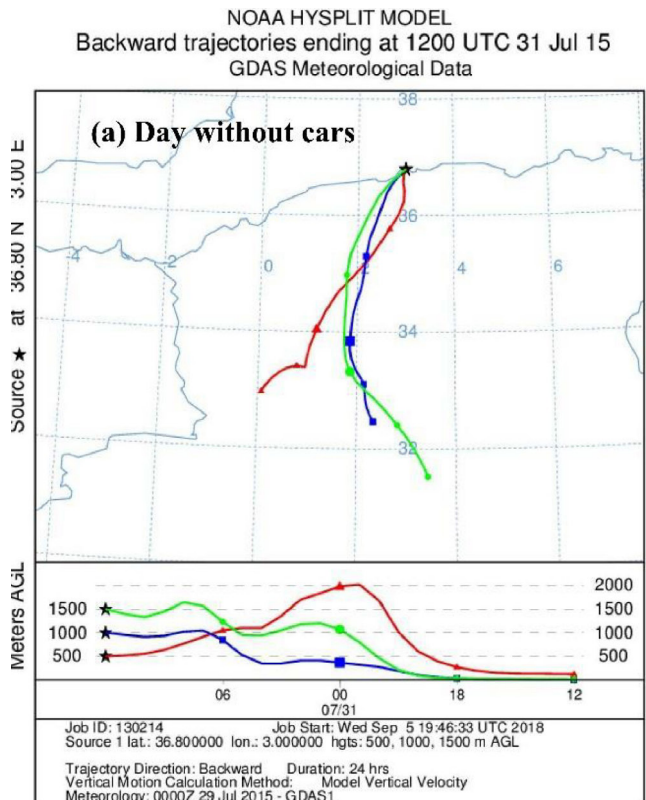
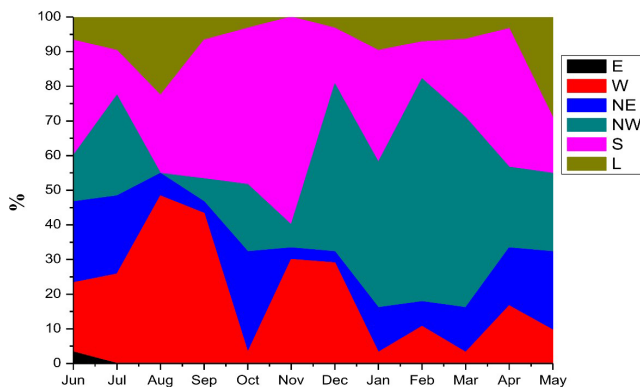


Figure 10: Back trajectories confirming pollution events (31 July and 7 August 2015).

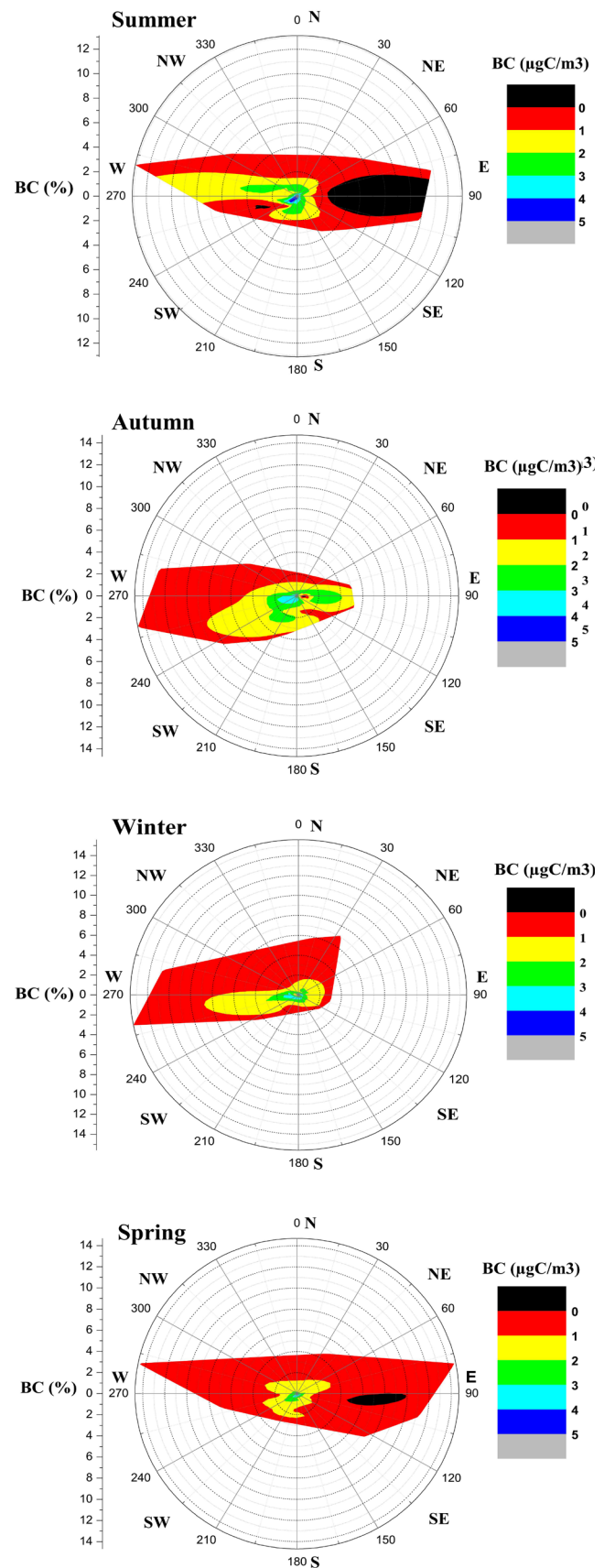


**Figure 11:** Wind sources map of the measurement site during one year of BC measurement.

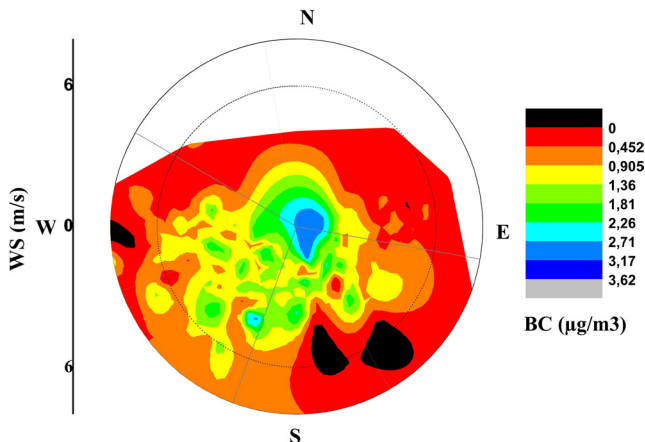
#### Annual source apportionment of black carbon

Figure 11 displays the variation of wind origin at 500m above ground level at the measurement site based on 365 air mass back trajectories performed using the Hysplit model for the year of the measurements. These maps are important for the interpretation of the high peaks of BC air pollution and their emission sources. From July to September 2014, the westerly sector was the main sector of wind origin, with average frequency of occurrence of 25.80% in July, 48.38% in August and 43.33% in September. In October and November 2014, the winds came mostly from the south with frequency of occurrence of 45.16% and 60.00%, respectively. For December 2014, January, February and March 2015, the principal source of winds was from north-west with frequencies of 48.38%, 41.93%, 64.28% and 54.84%, respectively. April was characterised by southerly winds coming from the Sahara, with frequency of occurrence of 40.00%. In May, the winds were local (29.03%), from the north-east (22.58%) and the north-west (22.58%).

The relationship between BC and the source apportionment of winds (measured by CHEMS network of CDER) for the four seasons of the measurement period is depicted in Figure 12. A filtering of the BC coming from the eight wind sectors has been performed. In summer, BC predominantly came from the west (23.94%), the south (24.89%) and the east (23.08%). The polluted air masses came from the west and north-west with mean concentrations reaching  $5 \mu\text{g m}^{-3}$  for southerly airflow and  $3 \mu\text{g m}^{-3}$  for westerly airflow; however, the air masses coming from the east were cleaner (concentrations below  $1 \mu\text{g m}^{-3}$ ). During the autumn, the predominant BC mass fraction directions were from the south (34.80%), the west (32.39%) and the east (12.96%), with BC mean concentrations reaching up to  $4 \mu\text{g m}^{-3}$  for the westerly and  $3 \mu\text{g m}^{-3}$  for the southerly and the easterly sectors. In the winter, the prevailing air masses came from the west (34.40%), the south (19.97%) and the north-west (13.10%). The BC mean concentrations coming from the west, the south and north-west reached up to 3, 3 and  $2 \mu\text{g m}^{-3}$ , respectively. In spring, BC mass fractions came mostly from the east (26.88%), the south (26.58%) and the west (22.88%). The BC mean concentrations reached up to  $3 \mu\text{g m}^{-3}$  for the southerly and  $2 \mu\text{g m}^{-3}$  for the easterly and the westerly sectors. Air masses rich in BC came from the west of Algiers.



**Figure 12:** Variation of BC versus the source apportionment of winds.

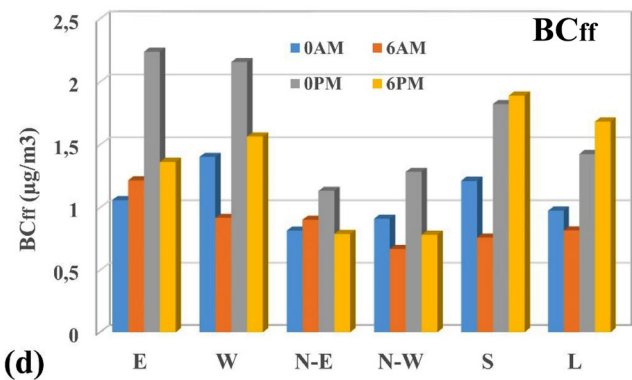
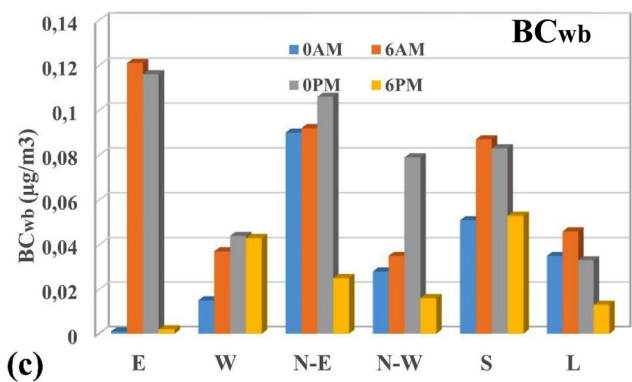
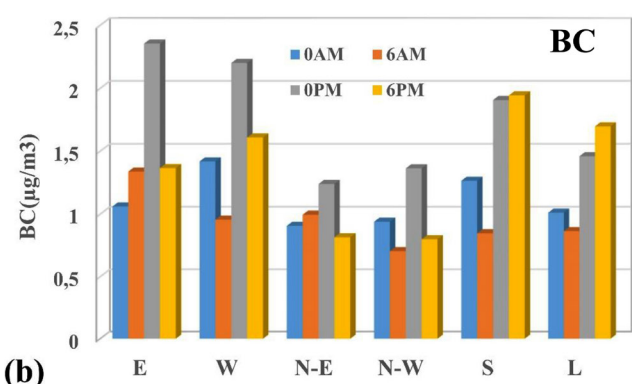
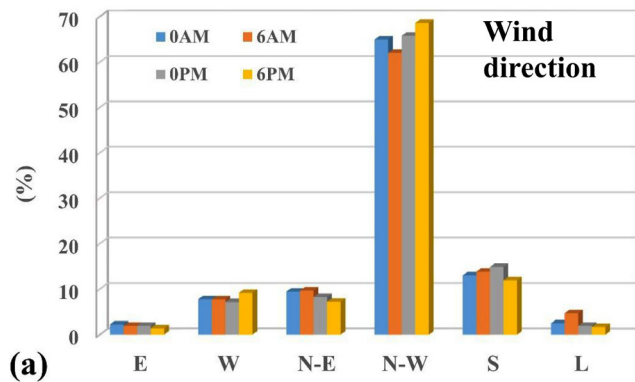


**Figure 13:** Variation of BC versus wind speed and wind direction for the entire sampling period.

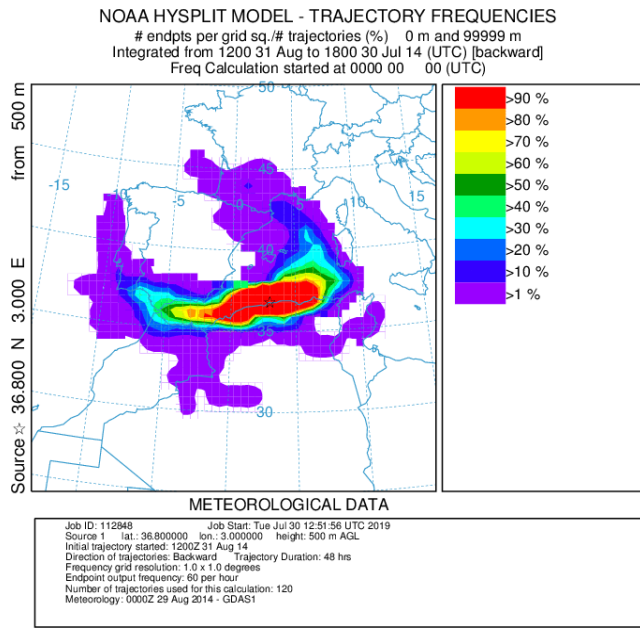
During the wet period, high BC mean concentrations of  $1.333 \mu\text{g}/\text{m}^3$  were recorded in association with southerly winds (petroleum industry), followed by local winds with  $1.238 \mu\text{g}/\text{m}^3$  (car fleet) despite the wet scavenging of BC. The highest mean concentrations of BC recorded during the dry period were from the easterly ( $1.380 \mu\text{g}/\text{m}^3$ ) and westerly ( $1.377 \mu\text{g}/\text{m}^3$ ) directions, coinciding with the emissions from the fires, harbour and airport to the east and petroleum refinery to the west.

Figure 13 displays a non-parametric wind regression analysis involving wind speed and source apportionment of winds (measured by CHEMS network of CDER) and BC concentrations, which could reveal more information on the source apportionment of BC. The mean concentration of BC was  $0.725 \mu\text{g}/\text{m}^3$  when ws was higher than  $4 \text{ m s}^{-1}$ ; however, it reached  $1.806 \mu\text{g}/\text{m}^3$  for ws lower than  $2 \text{ m s}^{-1}$ , reflecting the dispersion of BC by winds. Figure 13 revealed also that the prevailing sources of BC were from the south, north-east and north-west with concentrations reaching up to  $3.170 \mu\text{g}/\text{m}^3$  recorded when the wind speed was lower than  $2 \text{ m s}^{-1}$ . However, despite southerly winds reaching  $4 \text{ m s}^{-1}$ , high levels of BC of up to  $3.170 \mu\text{g}/\text{m}^3$  have been recorded from the southerly direction, suggesting the emissions from the oil industry.

For a better understanding of the source apportionment of BC and its long-range transport pathways, a back trajectory cluster analysis has been performed. Hysplit 120-hour back trajectories arriving at the site every 6 hours for 365 days (from 1 June 2014 to 31 May 2015) were carried out. The 6-hour time intervals were centered around midnight (00:00), 06:00, 12:00 and 18:00. The trajectories arriving at the site at a height of 500m A.S.L., were performed by the model Hysplit developed by NOAA (Figure 14a) for the year of measurement. We defined six clusters (north-east, north-west, south, east, west and local) as performed by Kouvarakis et al. (2000). A percentage of wind sources for each one of the four intervals (00:00, 06:00, 12:00 and 18:00) was calculated, followed by the calculation of the average of BC,  $\text{BC}_{\text{ff}}$  and  $\text{BC}_{\text{wb}}$  for each cluster during the four intervals. The north-westerly direction was predominant with percentages reaching up to 69, 66, 65 and 62% at 18:00, 12:00, 00:00 and 06:00,



**Figure 14:** Variation of BC,  $\text{BC}_{\text{ff}}$  and  $\text{BC}_{\text{wb}}$  concentrations with back trajectory cluster analysis.



**Figure 15:** Backward trajectory frequency in summer (30 July-31 August) 2014 to Algiers site.

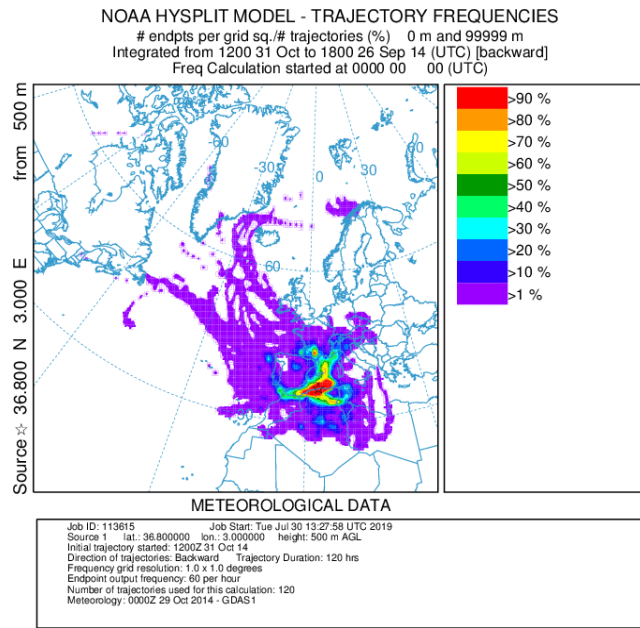


**Figure 16:** Backward trajectory frequency in autumn (September-October) 2014.

respectively, followed by the southerly direction with 15, 14, 13 and 12% at 12:00, 06:00, 00:00 and 18:00, respectively. These results confirm that the prevailing winds during the year of study were north-westerly followed by the southerly. Figures 14 b, c and d, display respectively the percentages of BC, BC<sub>ff</sub> and BC<sub>wb</sub> for the wind directions of the same four intervals during the year of measurements. For the midnight (00:00) cluster, the highest BC and BC<sub>ff</sub> mean concentrations were recorded from the west followed by the south with 1.417 and 1.402 µgm<sup>-3</sup> for BC and 1.263 and 1.212 µgm<sup>-3</sup> for BC<sub>ff</sub>, respectively, which can be explained by the presence of the oil refinery of Arzew in the west and the oil industry (pumping, processing, storage and transport) in the south. The highest mean concentrations of BC

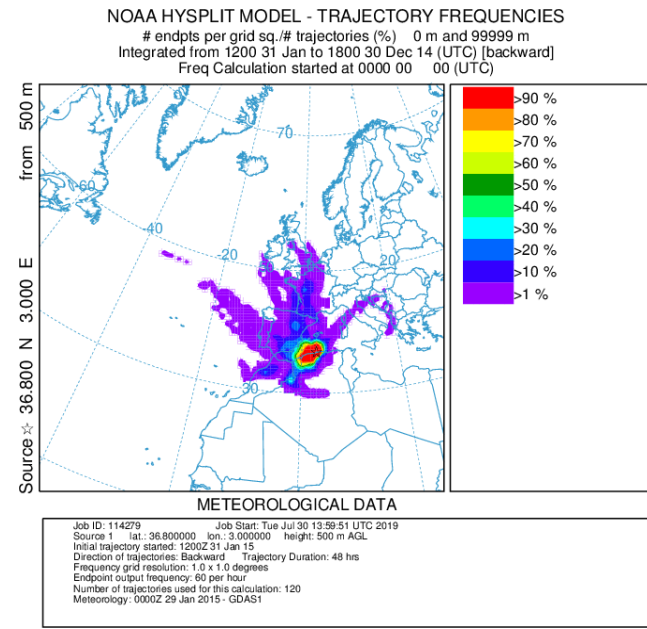


**Figure 17:** Backward trajectory frequency in winter (30 December 2014-31 January 2015) to Algiers site.

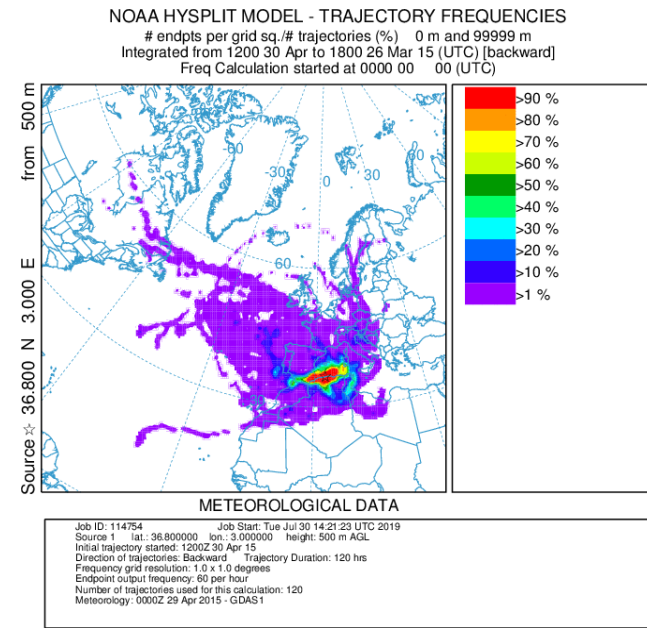


**Figure 18:** Backward trajectory frequency in spring (26 March-30 April) 2015 to Algiers site.

and BC<sub>ff</sub> observed for the 06:00 cluster came from the east and the north-east for BC with 1.336 and 0.994 µgm<sup>-3</sup>, respectively, and from the east and the west for BC<sub>ff</sub> with 1.215 and 0.917 µgm<sup>-3</sup>, respectively. The occurrence of such BC concentrations can be related to the harbor activities, the refineries to the east and west, the car fleet, and wood burning from Eastern Europe. With regards to the midnight (00:00) cluster, BC and BC<sub>ff</sub> sources were mainly from the east followed by the west with concentrations of 2.354 and 2.200 µgm<sup>-3</sup> for BC and 2.238 and 2.156 µgm<sup>-3</sup> for BC<sub>ff</sub>, respectively, which can be due to the harbor activities and petroleum refineries of Bejaia and Skikda in the east and of Arzew in the west.

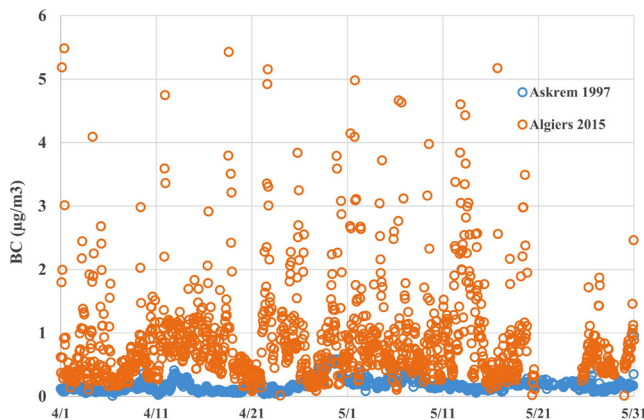


**Figure 19:** Comparison of BC concentrations at Algiers and Askrem stations.

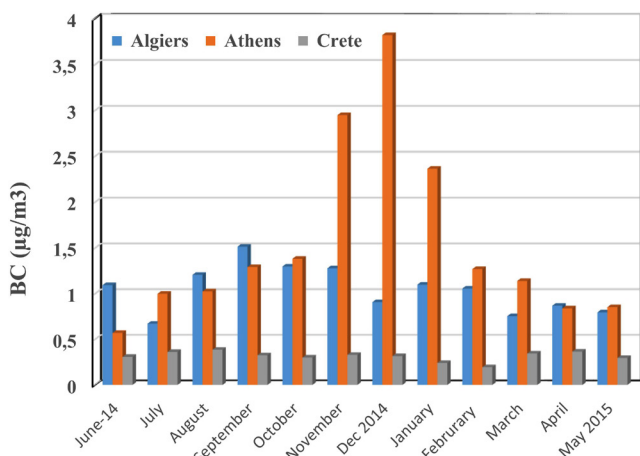


**Figure 20:** Comparison of monthly average BC concentrations at Algiers, Athens and Crete sites.

For the 18:00 cluster, the predominant BC and  $BC_{ff}$  mean concentrations were recorded from the south and in association with local airflow with 1.942 and  $1.696 \mu\text{gm}^{-3}$  for BC and 1.889 and  $1.683 \mu\text{gm}^{-3}$  for  $BC_{ff}$ , respectively, which can be due to the oil industry in the south and the local car fleet. For the case of  $BC_{wb}$  at midnight (00:00), the highest mean concentrations were predominantly from the north-east at  $0.090 \mu\text{gm}^{-3}$ , which is double the previous average, due to wood burning in Europe, followed by from the south at  $0.051 \mu\text{gm}^{-3}$ , close to the yearly mean, due to wild fires in the south of Algiers.

As to the 06:00 and midday clusters, the prevailing sources of  $BC_{wb}$  were to the east and the north-east with high means reaching up to  $0.121$  and  $0.092 \mu\text{gm}^{-3}$ , and  $0.116$  and  $0.106 \mu\text{gm}^{-3}$ , respectively, explained by wood burning in Eastern Europe and Tunisia. Finally, for the 18:00 cluster, the  $BC_{wb}$  predominant mean concentrations were close to the annual average and came from the south with  $0.053 \mu\text{gm}^{-3}$  due to cooking in the southern Algeria cities and from the west with  $0.043 \mu\text{gm}^{-3}$ , very likely derived from cooking in the western Algeria cities and from wood burning in Morocco.

For a better interpretation of the previous results, trajectory frequency maps were performed by the Hysplit model. Figure

15 displays the trajectory frequency in summer (July-August), where winds came mainly from the north-east and north-west, which is in line with the previous results bringing  $BC_{ff}$  and  $BC_{wb}$  emitted by fires and human activities.

Figure 16 presents the trajectory frequency map during autumn months (September-October) 2014. The prevailing winds were from the west, the south and the north-east, reinforcing the results presented in the meteorological map.

Figure 17 displays the trajectory frequency map in winter (December 2014-January 2015). The predominant winds were from the west, the south and the north-east, reinforcing the results presented in the meteorological map (Figure 11).

The trajectory frequency map during spring months (March-April) 2015 is shown in Figure 18. The prevailing winds during spring were from the north-east, the north-west and the south, which is in line with the previous results.

#### Anthropogenic sources of BC

We further focus on the anthropogenic part of BC emissions. For this purpose, a comparison of the levels of BC recorded in Algiers, Athens, Crete and Tamanrasset (the GAW/WMO reference station of Askrem) was performed.

Figure 19 displays the mean concentrations of BC recorded in Askrem, a background station situated at  $23.27^\circ\text{N}, 5.63^\circ\text{E}$  and an altitude of 2730 m a.s.l, from April and May 1997. In contrast to the mean BC concentration measured in Algiers during April-May 2015, i.e.,  $0.936 \mu\text{gm}^{-3}$ , the BC mean concentration recorded at the Askrem GAW station was  $0.168 \mu\text{gm}^{-3}$ . The BC concentrations in Algiers, which is heavily impacted by anthropogenic emissions, were 79.78% higher than at the Askrem background station.

Figure 20 shows a comparison of BC recorded in Algiers, Athens and Finokalia, Crete (Greece) during the year of measurement. The measurement site of Thissio (Athens), is situated in a city near the Akropolis, which is a much-visited museum. The Finokalia station is a background site used as a reference for Greek and European stations, 80 km east of Heraklion (Crete). The monthly average of BC in the urban agglomeration of Athens were similar to those recorded in Algiers, except in November, December and January, when the average concentrations were for Athens and Algiers respectively  $2.949$  and  $1.278$ ,  $3.819$  and  $0.907$  and  $2.364$  and  $1.099 \mu\text{gm}^{-3}$ . The high BC concentrations in Athens during winter could be due to wood burning for heating. The monthly mean BC levels observed at the background station of Finokalia, Crete varied mostly between  $0.2$  and  $0.5 \mu\text{gm}^{-3}$  with an annual average of  $0.314 \mu\text{gm}^{-3}$ , which represents 20.36% and 28.16% of the annual averages recorded in Athens and Algiers, respectively.

#### BC modelling

We further compare the observed BC with modelled results. For this, we used the TM4-ECPL global model developed by

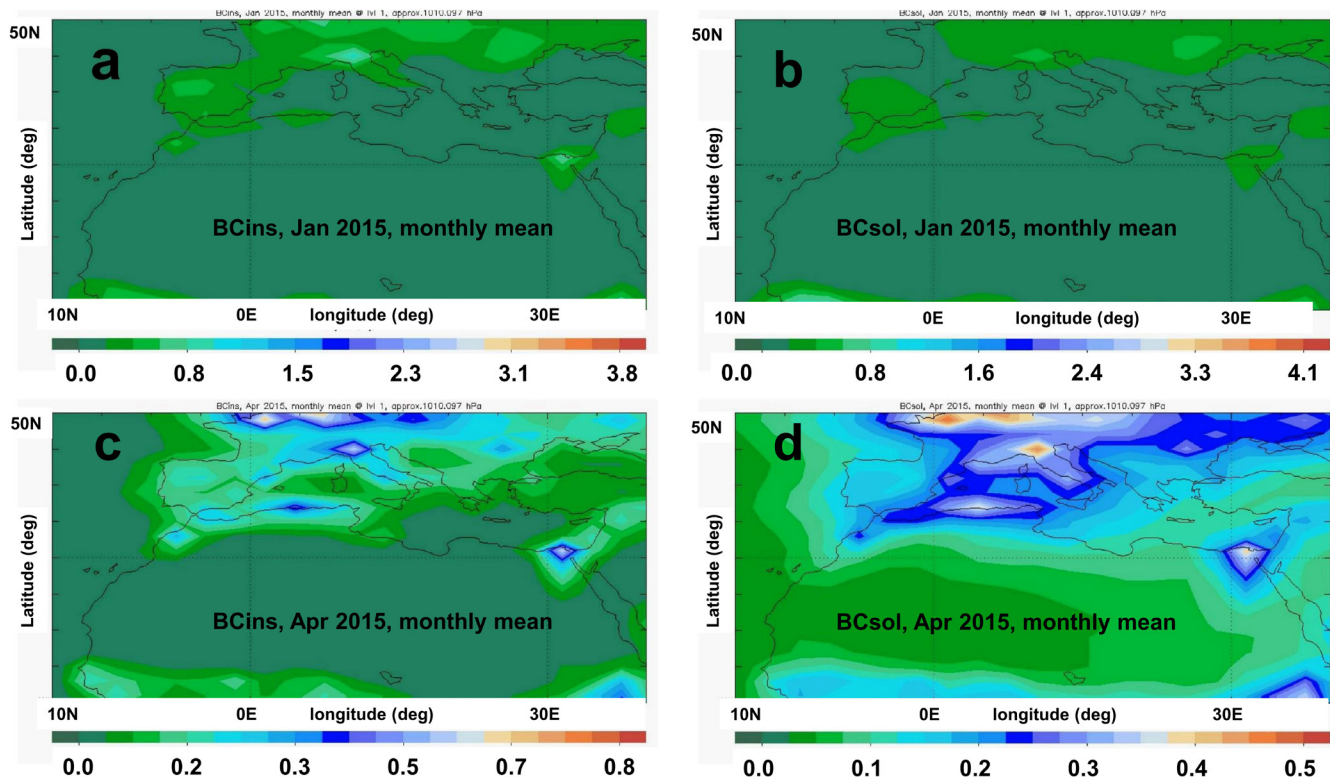


Figure 21: Variation of  $BC_{ins}$  and  $BC_{sol}$  in January and April 2015 using TM4-ECPL global model.

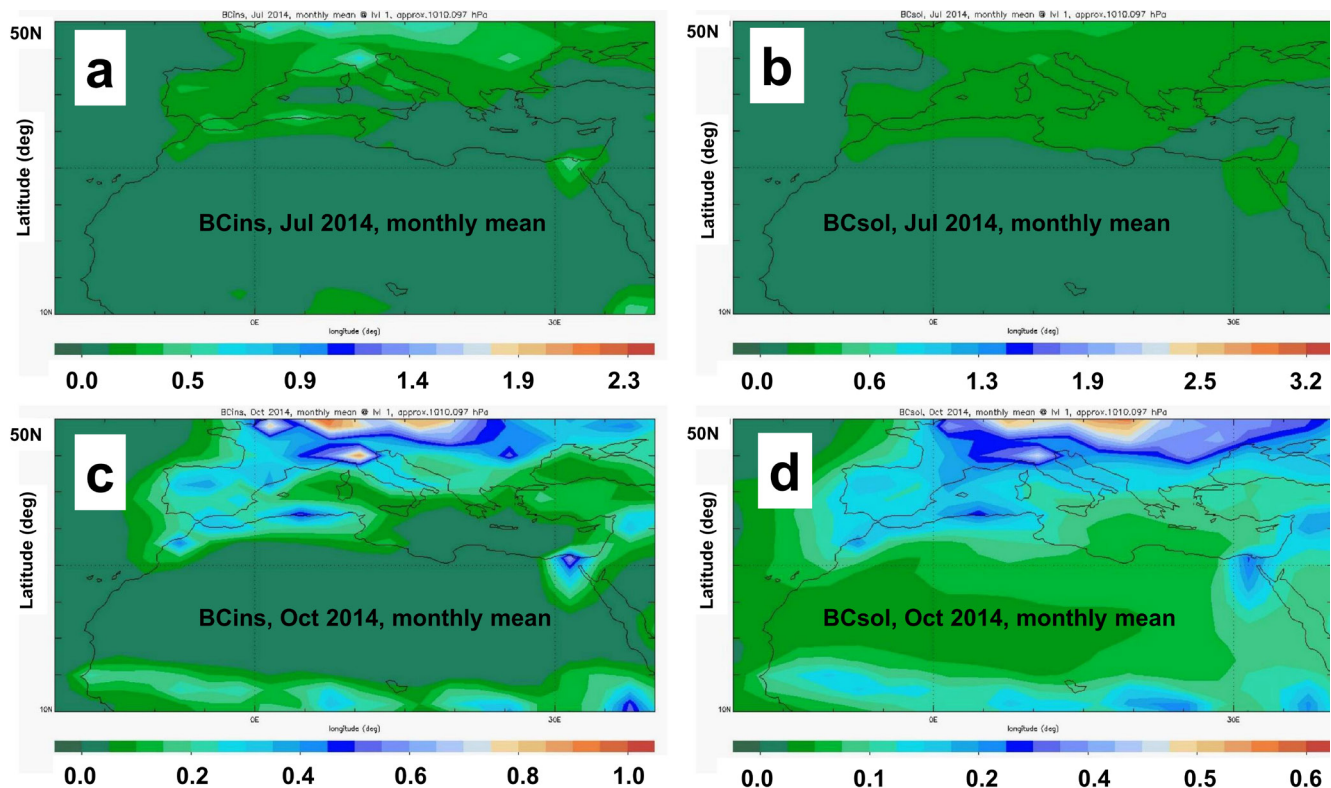


Figure 22: Monthly average concentrations of  $BC_{ins}$  and  $BC_{sol}$  in July and October 2014 modelled with TM4-ECPL.

the University of Crete (Greece). The model, which has been described in detail by Daskalakis et al. (2015), accounts for multiphase chemistry as well as all major aerosol types, including carbonaceous aerosols, both insoluble ( $BC_{ins}$ ) and soluble ( $BC_{sol}$ ) black carbon. The modelling of  $BC_{sol}$  and  $BC_{ins}$  is important to follow the atmospheric concentrations of fresh insoluble BC ( $BC_{ins}$ ) and the aged soluble BC ( $BC_{sol}$ ) that can be transported to the soil and ground water by wet scavenging. The results of the modeling are depicted in Figures 21 and 22 for July and October 2014 and January and April 2015, respectively. The months were chosen for a representative comparison of measured and modeled results for each month in the middle of each season. Figures 21a, b, c and d present the modeled  $BC_{ins}$  in January 2015,  $BC_{sol}$  in January 2015,  $BC_{ins}$  in April 2015 and  $BC_{sol}$  in April 2015, respectively. Figures 22a, b, c and d depict the modeled  $BC_{ins}$  in July 2014,  $BC_{sol}$  in July 2014,  $BC_{ins}$  in October 2014 and  $BC_{sol}$  in October 2014, respectively.  $BC_{ins}$  and  $BC_{sol}$  were higher in the center of Africa and the north of Europe, due to forest fires and wood burning. The modelled  $BC_{ins}$  and  $BC_{sol}$  in Algiers were respectively 0.50 and 0.30  $\mu\text{g m}^{-3}$  in July 2014, 0.50 and 0.40  $\mu\text{g m}^{-3}$  in October 2014, 0.40 and 0.40  $\mu\text{g m}^{-3}$  in January 2015 and 0.45 and 0.40  $\mu\text{g m}^{-3}$  in April 2015. Therefore, the total modelled BC for the four months was 0.80, 0.90, 0.80 and 0.85  $\mu\text{g m}^{-3}$ , respectively, which were very close to the mean measured BC concentration levels (0.745, 1.308, 1.108 and 0.917  $\mu\text{g m}^{-3}$ ).

In order to follow the variation of  $BC_{ff}$  and  $BC_{wb}$  by using the model proposed by Zotter et al. (2016), a statistical study has been performed. This statistical study was based on replacing the Angstrom exponents  $\alpha_{ff}=1$  and  $\alpha_{wb}=2$ , used in the aethalometer model by  $\alpha_{ff}=0.90$  and  $\alpha_{wb}=1.682$  proposed by Zotter et al. (2016), followed by a calculation of the new seasonal BC,  $BC_{ff}$  and  $BC_{wb}$  average concentrations. A decrease of seasonal  $BC_{ff}$  of 9.15 and 7.08% in winter and autumn, respectively, was calculated using the Zotter et al. (2016) model, compared to an increase of  $BC_{wb}$  of 96.97 and 90.43% for spring and autumn, respectively. This result indicates that  $BC_{wb}$  was undervalued by the model applied in our study, in contrary to the Zotter et al. (2016) model especially in spring and autumn.

### Angstrom exponent

Another important factor for the characterization of the source of measured BC during the year of study is the Angstrom exponent ( $\alpha$ ). Favez et al., (2009) revealed a low spectral dependence of black carbon light absorption ( $\alpha \sim 1$ ), in contrast, it is much higher for other aerosol components, i.e. hematite and brown carbon. Sandradewi et al. (2008) recorded light absorption exponents of 1.1 for traffic and 1.8–1.9 for wood burning, calculated from the light absorption at 470 and 950 nm. Soni et al. (2011) observed minimum values of the Angstrom exponent during May and maximum values during the winter period (December and January), related to a gradual decrease in the coarse particle concentration from summer to winter months. The Angstrom exponent (calculated at 470 and 950 nm) shown in Figure 23 varied mostly between 0.5 and 1.5 with an annual

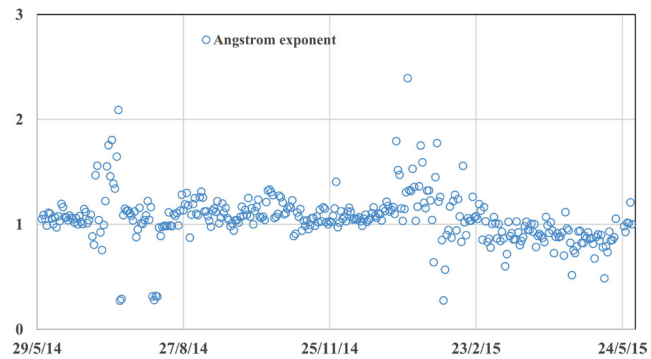


**Figure 23:** Daily variation of Angstrom exponent during the year of measurement at Algiers site.

average of 1.07, indicating that the main source of BC during the year of measurement was from fossil fuel burning, in line with the findings presented in this investigation.

### Mass absorption cross-section

The mass absorption cross-section (MAC) is also a good indicator of the source and the aging of BC particles. The MAC values are related to the aerosol mixing state, size, and morphology (Bond and Bergstrom, 2006), and increase with coating thickness or water at high relative humidity (Schnaiter, 2005). Laborde et al. (2013) revealed that the MAC average was  $\sim 7.3 \text{ m}^2 \text{ g}^{-1}$  for traffic emissions due to refractory BC (rBC) cores which are mainly uncoated and small. However, for the case of wood burning, the MAC average was  $\sim 7.8 \text{ m}^2 \text{ g}^{-1}$  explained by thicker coating and bigger rBC core size. Higher average MAC ( $\sim 8.8 \text{ m}^2 \text{ g}^{-1}$ ) were recorded with aged aerosols because of the thicker coating compared to aerosols from traffic and wood burning (Schnaiter, 2005). Cao et al. (2015) reported median MAC values of 20.0, 33.7, 29.1 and 27.6  $\text{m}^2 \text{ g}^{-1}$  during the spring, summer, autumn and winter, respectively, in China. However, the seasonal means of MAC values recorded in Switzerland were much smaller with 8.9, 9.5, 10.9, and 9.9  $\text{m}^2 \text{ g}^{-1}$  in spring, summer, autumn and winter, respectively (Lavanchy et al., 1999). The high MAC values recorded in China could be due to biomass burning, relatively large increase in the symmetrical particles and cluster-like structures emitted by motor vehicles, and the secondary and aged aerosols under high relative humidity (60–80%) and strong solar radiation.

In the present study, the seasonal means of MAC during summer, autumn, winter and spring were 10.97, 15.56, 30.27 and 17.12  $\text{m}^2 \text{ g}^{-1}$ , respectively. These high MAC values could be due to aged aerosols coming from Europe and secondary aerosols under high humidity and strong solar radiation, considering that the seasonal relative humidity was 58.38, 61.78, 64.12 and 62.03% in summer, autumn, winter and spring, respectively. The highest monthly averages for MAC were recorded in February, December and March at 36.18, 30.54 and 26.92  $\text{m}^2 \text{ g}^{-1}$ , respectively, when, relative humidity was high, reaching 63.94, 65.44 and 65.44%, respectively. The lowest MACs were recorded in July, September and October at 9.61, 1.75 and 11.88  $\text{m}^2 \text{ g}^{-1}$ , respectively, with

lower relative humidity of 58.00, 58.77 and 55.53%, respectively. This difference between the monthly variations in MAC could also be due to the clear skies in February and March especially, in contrast to the other months, and the wind in winter months bringing aged aerosols. July and September were also characterized by fresh aerosols due to wild fires as presented in the previous sections.

## Conclusions

Observations of BC,  $BC_{ff}$  and  $BC_{wb}$  over one year of measurement were performed for the first time in Algeria in order to better understand the levels, the occurrence, the sources and the seasonal modulations of BC air pollution. Hourly, diurnal, and seasonal variations in BC levels have been investigated. BC sources were found to be associated with traffic, wild fires, and the oil industry in the south of Algeria. Celebration events and long-range transport of pollution from Europe and neighboring countries have also been investigated.

The main source of BC pollution in Algiers city was found to be fossil fuel combustion accounting for 95.60% of the total annual mean BC levels, whereas  $BC_{wb}$  contributed only 4.40%.

The highest seasonal mean concentrations were recorded in summer and autumn at 1.283 and 1.209  $\mu\text{gm}^{-3}$  for BC and 1.217 and 1.177  $\mu\text{gm}^{-3}$  for  $BC_{ff}$ , respectively. The lowest mean concentrations were recorded in winter and spring at 1.023 and 0.966  $\mu\text{gm}^{-3}$  for BC and 0.933 and 0.956  $\mu\text{gm}^{-3}$  for  $BC_{ff}$ , respectively.

For  $BC_{wb}$ , the highest mean concentrations were reached in winter and summer at 0.090 and 0.066  $\mu\text{gm}^{-3}$ , respectively, due to the forest fires and long-range transport of air pollution from Europe. The lowest mean concentrations of  $BC_{wb}$  were recorded in autumn and spring at 0.032 and 0.010  $\mu\text{gm}^{-3}$ , respectively.

The BC pollution predominantly came from the west of Algiers, probably associated with the petroleum refinery in Arzew (Oran) situated 400 km from Algiers.

A source apportionment study of BC has been carried out for the wet and dry period of the studied year, followed by back trajectory cluster analysis for a better understanding of the long-range transport pathways. The highest BC mean concentrations of 1.333  $\mu\text{gm}^{-3}$  in the wet period were recorded in association with southerly winds, followed by local pollution contributing 1.238  $\mu\text{gm}^{-3}$  of BC. During the dry period, the highest mean concentrations of BC were observed in association with airflow from the East and West directions at concentrations of 1.380 and 1.377  $\mu\text{gm}^{-3}$  respectively.

The mass absorption cross-section (MAC) and Angstrom exponent were used to investigate the source and the ageing of BC measured in the present study.

The present study allowed a comparison of BC mean concentrations recorded in Algiers, Crete and Athens (Greece),

and Tamanrasset (GAW/WMO reference station of Askrem), revealing that the anthropogenic emissions were 79.78, 90.26 and 46.50% higher than at the Askrem background station for Algiers, Athens and Crete, respectively.

The annual average BC concentration recorded at the Algiers Observatory (suburban site) was much lower than that recorded in Anantapur (India), Prague (Czech), Athens (Greece) and Rome (Italy), but was higher than values measured in Santa Cruz de Tenerife (Spain), Crete (Greece) and Finland.

## Acknowledgements

We gratefully acknowledge the NOAA Air Resources Laboratory (ARL) for the provision of the HYSPLIT transport and dispersion model and READY website (<http://www.ready.noaa.gov>) used in this publication.

The authors are thankful to the National Meteorological Office, Algeria especially to Mr Mimouni Mohamed, for providing the Askrem data.

We thank also Dr Pavlos Zarmpas, Dr Georgos Kouvarakis, Georgos Fanourgakis and Dimitrios Amanatidis at the University of Crete (Greece) for their assistances with the modelling.

## References

- Ali, U., Syed, J.H., Junwen, L., Sánchez-García, L., Malik, R.N., Chaudhry, M.J.I., Arshad, M., Li, J., Zhang, G., Jones, K.C. 2014, 'Assessing the relationship and influence of black carbon on distribution status of organochlorines in the coastal sediments from Pakistan', *Environmental Pollution* 190: 82–90. <https://doi.org/10.1016/j.envpol.2014.03.024>.
- Andreae, M.O., Gelencser, A. 2006, 'Black carbon or brown carbon? The nature of light-absorbing carbonaceous aerosols', *Atmospheric Chemistry and Physics* 6:3131-3148. <https://doi.org/10.5194/acpd-6-3419-2006>.
- Bahadur, R., Russell, L.M., Jacobson, M.Z., Prather, K., Nenes, A., Adams, P. and Seinfeld, J.H. 2012, 'Importance of composition and hygroscopicity of BC particles to the effect of BC mitigation on cloud properties: Application to California conditions: Effect of CV particles on clouds', *Journal of Geophysical Research: Atmospheres* 117(D9). <https://doi.org/10.1029/2011JD017265>.
- Begam, G.R., Vachaspati, C.V., Ahammed, Y.N., Kumar, K.R., Babu, S.S. and Reddy, R.R. 2016, 'Measurement and analysis of black carbon aerosols over a tropical semi-arid station in Kadapa, India', *Atmospheric Research*, 171:77–91. <https://doi.org/10.1016/j.atmosres.2015.12.014>.
- Bond, T.C. and Bergstrom, R.W. 2006, 'Light Absorption by Carbonaceous Particles: An Investigative Review', *Aerosol Science and Technology* 40(1):27–67. <https://doi.org/10.1080/02786820500421521>.

- Bond, T. C., Doherty, S. J., Fahey, D. W., Forster, P. M., Berntsen, T., DeAngelo, B. J., Flanner, M. G., Ghan, S., Kärcher, B., Koch, D., Kinne, S., Kondo, Y., Quinn, P. K., Sarofim, M. C., Schultz, M. G., Schulz, M., Venkataraman, C., Zhang, H., Zhang, S., Bellouin, N., Guttikunda, S. K., Hopke, P. K., Jacobson, M. Z., Kaiser, J. W., Klimont, Z., Lohmann, U., Schwarz, J. P., Shindell, D., Storelvmo, T., Warren, S. G. and Zender, C. S. 2013, 'Bounding the role of black carbon in the climate system: A scientific assessment', *Journal of Geophysical Research* 118(11): 5380–5552. <https://doi.org/10.1002/jgrd.50171>.
- Byčenkiene, S., Ulevicius, V. and Kecorius, S. 2011, 'Characteristics of black carbon aerosol mass concentration over the East Baltic region from two-year measurements', *Journal of Environmental Monitoring* 13(4):1027. <https://doi.org/10.1039/c0em00480d>.
- Cao, J., Zhu, C., Ho, K., Han, Y., Shen, Z., Zhan, C. and Zhang, J. 2015, 'Light attenuation cross-section of black carbon in an urban atmosphere in northern China', *Particuology* 18:89–95. <https://doi.org/10.1016/j.partic.2014.04.011>
- Cheng, Y., Lee, S.C., Ho, K.F., Wang, Y.Q., Cao, J.J., Chow, J.C. and Watson, J.G. 2006, 'Black carbon measurement in a coastal area of south China', *Journal of Geophysical Research* 111(D12). <https://doi.org/10.1029/2005JD006663>.
- Cheng, Y.-H., Liao, C.-W., Liu, Z.-S., Tsai, C.-J. and Hsi, H.C. 2014, 'A size-segregation method for monitoring the diurnal characteristics of atmospheric black carbon size distribution at urban traffic sites', *Atmospheric Environment* 90:78–86. <https://doi.org/10.1016/j.atmosenv.2014.03.023>.
- Chiloane, K. E., Beukes, J. P., van Zyl, P. G., Maritz, P., Vakkari, V., Josipovic, M., Venter, A. D., Jaars, K., Tiitta, P., Kulmala, M., Wiedensohler, A., Liousse, C., Mkhathwana, G. V., Ramandh, A. and Laakso, L. 2017, Spatial, temporal and source contribution assessments of black carbon over the northern interior of South Africa, *Atmos. Chem. Phys.* 17(10):6177–6196. <https://doi.org/10.5194/acp-17-6177-2017>.
- Daskalakis, N., Myriokefalitakis, S. and Kanakidou, M. 2015, 'Sensitivity of tropospheric loads and lifetimes of short lived pollutants to fire emissions', *Atmospheric Chemistry and Physics* 15(6):3543–3563. <https://doi.org/10.5194/acp-15-3543-2015>.
- De Miranda, R.M., de Fatima Andrade, M., Fornaro, A., Astolfo, R., de Andre, P.A. and Saldiva, P. 2012, 'Urban air pollution: a representative survey of PM<sub>2.5</sub> mass concentrations in six Brazilian cities', *Air Quality, Atmosphere & Health* 5(1):63–77. <https://doi.org/10.1007/s11869-010-0124-1>.
- Favez, O., Cachier, H., Sciare, J., Sarda-Estève, R., Martinon, L. 2009, 'Evidence for a significant contribution of wood burning aerosols to PM<sub>2.5</sub> during the winter season in Paris, France', *Atmospheric Environment* 43:3640–3644. <https://doi.org/10.1016/j.atmosenv.2009.04.035>.
- Gadham, H. and Jayaraman, A. 2010, 'Absorbing aerosols: contribution of biomass burning and implications for radiative forcing', *Annales Geophysicae* 28(1):103–111. <https://doi.org/10.5194/angeo-28-103-2010>.
- Hooda, R. K., Kivekäs, N., O'Connor, E. J., Collaud Coen, M., Pietikäinen, J.-P., Vakkari, V., Backman, J., Henriksson, S. V., Asmi, E., Komppula, M., Korhonen, H., Hyvärinen, A.-P. and Lihavainen, H. 2018, 'Driving factors of aerosol properties over the foothills of Central Himalayas based on 8.5 years continuous measurements', *J. Geophys. Res. Atmos.* 123(23):13421–13442. <https://doi.org/10.1029/2018JD029744>.
- Jennings, S.G., Spain, T.G., Doddridge, B.G., Maring, H., Kelly, B.P. and Hansen, A.D.A. 1996, 'Concurrent measurements of black carbon aerosol and carbon monoxide at Mace Head', *Journal of Geophysical Research: Atmospheres* 101(D14):19447–19454. <https://doi.org/10.1029/96JD00614>.
- Jose, S., Niranjan, K., Gharai, B., Rao, P.V.N. and Nair, V.S. 2016, 'Characterisation of absorbing aerosols using ground and satellite data at an urban location, Hyderabad', *Aerosol and Air Quality Research* 16( 6): 1427–1440. <https://doi.org/10.4209/aaqr.2014.09.0220>.
- Krecl, P., Targino, A.C. and Johansson, C. 2011, 'Spatiotemporal distribution of light-absorbing carbon and its relationship to other atmospheric pollutants in Stockholm', *Atmospheric Chemistry and Physics* 11(22):11553–11567. <https://doi.org/10.5194/acp-11-11553-2011>.
- Laborde, M., Crippa, M., Tritscher, T., Jurányi, Z., Decarlo, P.F., Temime-Roussel, B., Marchand, N., Eckhardt, S., Stohl, A., Baltensperger, U., Prévôt, A.S.H., Weingartner, E., Gysel, M. 2013, 'Black carbon physical properties and mixing state in the European megacity Paris', *Atmospheric Chemistry and Physics* 13(11):5831–5856. <https://doi.org/10.5194/acp-13-5831-2013>.
- Lavanchy, V.M.H., Gäggeler, H.W., Nyeki, S. and Baltensperger, U. 1999, 'Elemental carbon (EC) and black carbon (BC) measurements with a thermal method and an aethalometer at the high-alpine research station Jungfraujoch', *Atmospheric Environment* 33(17):2759–2769. [https://doi.org/10.1016/S1352-2310\(98\)00328-8](https://doi.org/10.1016/S1352-2310(98)00328-8).
- Lohmann, R., MacFarlane, J.K. and Gschwend, P.M. 2005, 'Importance of black carbon to sorption of native PAHs, PCBs, and PCDDs in Boston and New York harbor sediments', *Environmental Science & Technology* 39(1):141–148. <https://doi.org/10.1021/es049424+>.
- Mahmoud, K.F., Alfaro, S.C., Favez, O., Abdel Wahab, M.M. and Sciare, J. 2008, 'Origin of black carbon concentration peaks in Cairo (Egypt)', *Atmospheric Research* 89(1–2):161–169. <https://doi.org/10.1016/j.atmosres.2008.01.004>.

- Masiello, C.A. and Druffel, E.R.M. 1998, 'Black carbon in deep-sea sediments', *Science*, New Series 280(5371):1911–1913. <https://doi.org/10.1126/science.280.5371.1911>.
- Nair, V.S., Moorthy, K.K., Alappattu, D.P., Kunhikrishnan, P.K., George, S., Nair, P.R., Babu, S.S., et al. 2007, 'Wintertime aerosol characteristics over the Indo-Gangetic Plain (IGP): Impacts of local boundary layer processes and long-range transport: Winter aerosols over Indo-Gangetic Plain', *Journal of Geophysical Research: Atmospheres* 112(D13). <https://doi.org/10.1029/2006JD008099>.
- Pu, W., Wang, X., Zhang, X., Ren, Y., Shi, J.-S., Bi, J.-R., Zhang, B.-D. 2015, 'Size distribution and optical properties of particulate matter ( $PM_{10}$ ) and black carbon (BC) during dust storms and local air pollution events across a loess plateau site', *Aerosol and Air Quality Research*, 15(6): 2212–2224. <https://doi.org/10.4209/aaqr.2015.02.0109>.
- Ramachandran, S. and Rajesh, T.A. 2007, 'Black carbon aerosol mass concentrations over Ahmedabad, an urban location in western India: Comparison with urban sites in Asia, Europe, Canada, and the United States', *Journal of Geophysical Research* 112(D6). <https://doi.org/10.1029/2006JD007488>.
- Reche, C., Querol, X., Alastuey, A., Viana, M., Pey, J., Moreno, T., Rodríguez, S., et al. 2011, 'New considerations for PM, Black Carbon and particle number concentration for air quality monitoring across different European cities', *Atmospheric Chemistry and Physics* 11(13):6207–6227. <https://doi.org/10.5194/acp-11-6207-2011>.
- Reddy, B.S.K., Kumar, K.R., Balakrishnaiah, G., Gopal, K.R., Reddy, R.R., Reddy, L.S.S., Ahammed, Y.N., Narasimhulu, K., Moorthy, K.K., Babu, S.S. 2012, 'Potential source regions contributing to seasonal variations of black carbon aerosols over Anantapur in Southeast India', *Aerosol and Air Quality Research* 12(3):344–358. <https://doi.org/10.4209/aaqr.2011.10.0159>.
- Saarikoski, S., Timonen, H., Saarnio, K., Aurela, M., Järvi, L., Keronen, P., Kerminen, V.-M., Hillamo, R. 2008, 'Sources of organic carbon in fine particulate matter in northern European urban air', *Atmospheric Chemistry and Physics* 8(20):6281–6295. <https://doi.org/10.5194/acp-8-6281-2008>.
- Saha, A. and Despiau, S. 2009, 'Seasonal and diurnal variations of black carbon aerosols over a Mediterranean coastal zone', *Atmospheric Research* 92(1):27–41. <https://doi.org/10.1016/j.atmosres.2008.07.007>.
- Salcedo, D., Onasch, T.B., Dzepina, K., Canagaratna, M.R., Zhang, Q., Huffman, J.A., DeCarlo, P.F., Jayne, J.T., Mortimer, P., Worsnop, D.R., Kolb, C.E., Johnson, K.S., Zuberi, B., Marr, L.C., Volkamer, R., Molina, L.T., Molina, M.J., Cardenas, B., Bernabé, R.M., Márquez, C., Gaffney, J.S., Marley, N.A., Laskin, A., Shutthanandan, V., Xie, Y., Brune, W., Lesher, R., Shirley, T., Jimenez, J.L. 2006, "Characterization of ambient aerosols in Mexico City during the MCMA-2003 campaign with Aerosol Mass Spectrometry: results from the CENICA Supersite", *Atmospheric Chemistry and Physics* 6(4):925–946. <https://doi.org/10.5194/acp-6-925-2006>.
- Sandradewi, J., Pre'vo't, A.S.H., Szidat, S., Perron, N., Alfara, M.R., Lanz, V.A., Weingartner, E., Baltensperger, U., 2008b. Using aerosol light absorption measurements for the quantitative determination of wood burning and traffic emission contributions to particulate matter. *Environmental Science and Technology* 42:3316–3323. <https://doi.org/10.1021/es702253m>.
- Schnaiter, M. 2005, 'Absorption amplification of black carbon internally mixed with secondary organic aerosol', *Journal of Geophysical Research*, 110(D19). <https://doi.org/10.1029/2005JD006046>.
- Sciare, J., d'Argouges, O., Sarda-Estève, R., Gaimoz, C., Dolgorouky, C., Bonnaire, N., Favez, O., Bonsang, B., Gros, V. 2011, 'Large contribution of water-insoluble secondary organic aerosols in the region of Paris (France) during wintertime: Wintertime water-insoluble SOA', *Journal of Geophysical Research: Atmospheres* 116(D22). <https://doi.org/10.1029/2011JD015756>.
- Seidel, D.J. and Birnbaum, A.N. 2015, 'Effects of Independence Day fireworks on atmospheric concentrations of fine particulate matter in the United States', *Atmospheric Environment*, 115:192–198. <https://doi.org/10.1016/j.atmosenv.2015.05.065>.
- Seinfeld, J.H. and Pandis, S.N. 2006, 'Atmospheric Chemistry and Physics: From Air Pollution to Climate Change, 2. ed.', Hoboken, NJ.
- Singla, V., Mukherjee, S., Kashikar, A.S., Safai, P.D. and Pandithurai, G. 2019, 'Black carbon: source apportionment and its implications on CCN activity over a rural region in Western Ghats, India', *Environmental Science and Pollution Research*, 26(7):7071–7081. <https://doi.org/10.1007/s11356-019-04162-w>.
- Streets, D.G., Gupta, S., Waldhoff, S.T., Wang, M.Q., Bond, T.C. and Yiyun, B. 2001, 'Black carbon emissions in China', *Atmospheric Environment* 35(25): 4281–4296. [https://doi.org/10.1016/S1352-2310\(01\)00179-0](https://doi.org/10.1016/S1352-2310(01)00179-0).
- Targino, A.C. and Krecl, P. 2017, 'Local and Regional Contributions to Black Carbon Aerosols in a Mid-Sized City in Southern Brazil', *Aerosol and Air Quality Research* 16(1):125–137. <https://doi.org/10.4209/aaqr.2015.06.0388>.
- Venkatachari, P., Zhou, L., Hopke, P.K., Felton, D., Rattigan, O.V., Schwab, J.J. and Demerjian, K.L. 2006, 'Spatial and temporal variability of black carbon in New York City: SPATIAL AND TEMPORAL VARIATIONS OF BC', *Journal of Geophysical Research: Atmospheres* 111(D10). <https://doi.org/10.1029/2005JD006314>.

Vodička, P., Schwarz, J. and Ždímal, V. 2013, 'Analysis of one year's OC/EC data at a Prague suburban site with 2-h time resolution', *Atmospheric Environment* 77:865–872. <https://doi.org/10.1016/j.atmosenv.2013.06.013>.

Wang, H., Nie, L., Liu, D., Gao, M., Wang, M. and Hao, Z. 2015, 'Physico-chemical characterization and source tracking of black carbon at a suburban site in Beijing', *Journal of Environmental Sciences* 33:188–194. <https://doi.org/10.1016/j.jes.2015.05.001>.

Weingartner, E., et al. (2003), Absorption of Light by Soot Particles: Determination of the Absorption Coefficient by Means of Aethalometers *Journal of Aerosol Science* 34:1445–1463. [https://doi.org/10.1016/S0021-8502\(03\)00359-8](https://doi.org/10.1016/S0021-8502(03)00359-8).

Wu, D., Wu, C., Liao, B., Chen, H., Wu, M., Li, F., Tan, H., Deng, T., Li, H., Jiang, D., Yu, J.Z. 2013, 'Black carbon over the South China Sea and in various continental locations in South China', *Atmospheric Chemistry and Physics* 13(24):12257–12270. <https://doi.org/10.5194/acp-13-12257-2013>.

Zotter, P., Herich, H., Gysel, M., El-Haddad, I., Zhang, Y., Močnik, G., Hüglin, C., Baltensperger, U., Szidat, S., Prévôt, A.S.H. 2017, 'Evaluation of the absorption Ångström exponents for traffic and wood burning in the Aethalometer based source apportionment using radiocarbon measurements of ambient aerosol', *Atmospheric Chemistry and Physics* 17:4229–4249. <https://doi.org/10.5194/acp-2016-621>.